frontiers | Frontiers in Marine Science

TYPE Original Research
PUBLISHED 14 February 2023
DOI 10.3389/fmars.2023.1033710

OPEN ACCESS

EDITED BY
Libin Zhang,
Institute of Oceanology (CAS), China

REVIEWED BY
Gianna Innocenti,
University of Florence, Italy
Piero Cossu,
University of Sassari, Italy

*CORRESPONDENCE
Paolo Stara
paolostara@yahoo.it
Maria Cristina Follesa
follesac@unica.it
Rita Cannas
rcannas@unica.it

†These authors share first authorship

SPECIALTY SECTION
This article was submitted to Marine Biology, a section of the journal Frontiers in Marine Science

RECEIVED 31 August 2022
ACCEPTED 12 January 2023
PUBLISHED 14 February 2023

CITATION
Stara P, Melis R, Bellodi A, Follesa MC, Corradini C, Carugati L, Mulas A, Sibiriu M and Cannas R (2023) New insights on the systematics of echinoids belonging to the family Spatangidae Gray, 1825 using a combined approach based on morphology, morphometry, and genetics. *Front. Mar. Sci.* 10:1033710. doi: 10.3389/fmars.2023.1033710

New insights on the systematics of echinoids belonging to the family Spatangidae Gray, 1825 using a combined approach based on morphology, morphometry, and genetics

Paolo Stara[1*†], Riccardo Melis[2†], Andrea Bellodi[2†], Maria Cristina Follesa[2*], Carlo Corradini[3], Laura Carugati[2], Antonello Mulas[2], Michela Sibiriu[2] and Rita Cannas[2*]

[1]Centro Studi di Storia Naturale del Mediterraneo, Geomuseo Monte Arci, Masullas, Italy, [2]Department of Life and Environmental Sciences, University of Cagliari, Cagliari, Italy, [3]Dipartimento di Matematica e Geoscienze, Università di Trieste, Trieste, Italy

Spatangoids are probably the least resolved group within echinoids, with known topological incongruencies between phylogenies derived from molecular (very scarce) and morphological data. The present work, based on the analysis of 270 specimens of Spatangidae (Echinoidea, Spatangoida) trawled in the Sardinian seas (Western Mediterranean), allowed us to verify the constancy of some characters that we consider to be diagnostic at the genus level —such as the path of the subanal fasciole and the relationship between labrum and adjacent ambulacral plates —and to distinguish two distinct forms within the studied material. Based on morphological characters, morphometrics, and molecular analyses (sequencing of two mitochondrial markers: cytochrome *c* oxidase subunit1 (COI) and 16S), most of the individuals were classified as morphotype A and attributed to the species *Spatangus purpureus*, the most common spatangoid in the Mediterranean Sea, while a few corresponded to a different morphotype (B), genetically close to the species *Spatangus raschi*. Preliminary morphological analyses seemed to indicate that morphotype B specimens from Sardinia are slightly different from *S. raschi* and from *Spatangus subinermis* individuals, the second species of the family known to occur in the Mediterranean Sea. On the basis of morpho-structural observations and molecular analyses, comparing Mediterranean living forms with species from other areas (Central Eastern Atlantic, North Sea and neighboring basins, South African Sea, Philippines and Indonesian Archipelago, New Zealand, and Hawaiian Islands), the clear distinction of *S. purpureus* from several other species classified as *Spatangus* was confirmed. Based on the morphological and genetic differences, we propose to maintain the genus *Spatangus* including in it only the type species *S. purpureus* among the living species and to establish the new genus *Propespatagus* nov. gen. to include several other species previously classified as *Spatangus*. The clear distinction among different genera was also detected in fossil forms of *Spatangus*, *Propespatagus* nov. gen., and *Sardospatangus* (†) from the European Oligo-Miocene sedimentary rocks of Germany; the Miocene of Ukraine, Italy, and

North Africa; the Plio-Pleistocene of Italy; and the Mio-Pliocene of Florida (USA). The new data can help in addressing taxonomic ambiguities within echinoids, as well as in improving species identification, and hence biodiversity assessments in the Mediterranean region.

KEYWORDS

echinoids, *Propespatagus*, new genus, Mediterranean, DNA analyses, morphology, morphometrics

1 Introduction

Irregular sea urchins (Irregularia), predominantly infaunal and bilaterally symmetrical forms covered by small and specialized spines (Mongiardino Koch et al., 2022), are subdivided into Atelostomata (heart urchins and allies) and Neognathostomata (sand dollars, sea biscuits, and "cassiduloids") (Mongiardino Koch et al., 2022). Atelostomata are recognized as the most diverse of the clades of echinoids (Kroh, 2020). Thanks to their robust globular skeleton (the test), plenty of morphological data are available for both extant and extinct species (Kroh and Smith, 2010; Mongiardino Koch and Thompson, 2021). Despite this, studies on their systematics and diffusion in different oceans are sparse, apart from some important recent works (Smith and Stockley, 2005; Smith et al., 2006; Kroh and Smith, 2010; Ziegler et al., 2012 and citations therein), but many of them are relatively old (Mortensen, 1907; Clark, 1917; Mortensen, 1948; Mortensen, 1951; Serafy and Fell, 1985; Baker and Rowe, 1990, and citations therein). Furthermore, in addition to the descriptions based on morphological characters (Shin, 2013; Filander and Griffiths, 2017), there are only a few recent studies based on structural analysis (Sumida et al., 2001).

It has been demonstrated that fossil taxa improve phylogenetic analysis of morphological datasets, even when highly fragmentary (Mongiardino Koch, 2021).

Apart from morpho-structural data (from fossils and living species), genetic data could represent complementary resources for unraveling the phylogenetic relationships (Mongiardino Koch et al., 2022).

In general, these two approaches, morphological and molecular, have been developed largely in isolation, with very few studies integrating them. Moreover, conflicts between morphological and molecular evidence often provided unclear results (Smith et al., 2006; Kroh and Smith, 2010; Thompson et al., 2017; Mongiardino Koch et al., 2018). However, the continuous development of new data sets and methods has allowed for important recent advances. For instance, Kroh (2020) proposed a revised classification that incorporates results from morphological as well as phylogenetic and phylogenomic studies, suggesting that this classification could be further modified as taxon sampling of phylogenomic analyses increases, reducing the areas of conflict between morphological and molecular data. Mongiardino Koch and Thompson (2021) demonstrated that combining different data sources increases topological accuracy and helps resolve conflicts between molecular and morphological data. Similarly, Mongiardino Koch et al. (2022), using 18 novel genomes and transcriptomes to build a phylogenomic dataset with a near-complete sampling of major lineages, revised the phylogeny and divergence times of echinoids and place their history within the broader context of echinoderm evolution.

The present study focuses on irregular sea urchins of the family Spatangidae Gray, 1825, according to Smith and Kroh (2011) and Kroh and Mooi (2022), which includes three genera: *Spatangus* Gray, 1825, *Plethotaenia* H.L. Clark, 1917, and *Granopatagus* Lambert, 1915. The first genus is reported to be present all over the world, while the second is restricted to the Caribbean Sea (Mortensen, 1951; Néraudeau et al., 2010; Kroh and Mooi, 2022).

The third, *Granopatagus*, is controversial. According to Smith and Kroh (2011), it includes four species: two are extant species (*Granopatagus inermis* Mortensen, 1913, distributed in the Mediterranean and along the Atlantic-European coasts, and *Granopatagus paucituberculatus* (Agassiz & Clark, 1907) from Hawaii), while the other two are fossil species (*Granopatagus lonchophorus* (Meneghini, in Desor, 1858) and *Granopatagus subinermis* (Pomel, 1883)). On the contrary, according to Kroh and Mooi (2022), *Granopatagus* includes only the fossil species *Granopatagus loncophorus*, while the other three species are moved to the genus *Spatangus*, and the two distinct species *G. inermis* and *G. subinermis* unified as *Spatangus subinermis* (fossil+recent).

The distinctive characters of the genus *Granopatagus* were never fully described. Originally, Lambert (1915) proposed *Granopatagus* as a sub-genus of *Spatangus* on the basis of 1) a very deep sinus, 2) very short petals, and 3) the almost total lack of primary tubercles. However, these characters are not distinctive at a genus level; moreover, the type specimen used for the description, once kept in the Museum of the University of Pisa, is no longer available.

Recently, a further genus, *Sardospatangus* Stara, Charbonnier et Borghi, 2018, has been proposed by Stara et al. (2018). It is an extinct genus of which only fossil species are known in peri-mediterranean sedimentary rocks.

Based on previous reports, there are two extant species of Spatangidae present in the Mediterranean continental shelf and offshore: *Spatangus purpureus* Müller, 1776 (Figure S1), i.e., the type species of the genus *Spatangus*, and *S. subinermis* (*sensu* Kroh and Mooi, 2022).

To date, only a few reports or studies have been published on the Mediterranean populations of these two species (Risso, 1826; Mortensen, 1913; Bonnet, 1926; Tortonese, 1965; Borri et al., 1990).

To solve the numerous taxonomic uncertainties of this and other genera, starting from the middle of the last century, several researchers have been oriented toward the analysis of the pattern (scheme) of the plates composing the test (test plating) and on their fasciole pathways (Kroh, 2005; Smith and Stockley, 2005; Kroh, 2007; Stara et al., 2016; Stara et al., 2018).

Despite the observations on heterochrony previously published by Mc Namara (1982; 1987; 1988; 1989), where the authors reported a wide variability in the relationships between the plates (spatangoids not included in the studies), raising doubts about their use in systematic diagnostics, these characters proved to be valid. Smith and Stockley (2005), analyzing a large number of 89 species belonging to several genera, stated that the fasciole pathways are highly conservative, and therefore, the authors considered them distinctive characters of considerable phylogenetic (and systematic) importance. Similarly, Stara et al. (2018) considered the number of plates adjacent to the labrum and the shape, size, and reciprocal position of the plates that compose the oral face of spatangoids and spatangids as a set of highly diagnostic characters in systematic studies.

On the contrary, in the past, only rare comparative studies based on molecular analysis of spatangids were performed (Littlewood and Smith, 1995; Smith et al., 1995; Stockley et al., 2005; Smith et al., 2006; Kroh and Smith, 2010; Kroh, 2020).

The main goal of this work focused on the family Spatangidae, a group of spatangoids whose phylogenetic relationships are less resolved (Kroh, 2020), is to describe the spatangids collected in the Sardinian seas, to clearly identify the species collected, and to clarify their systematic position. The genus-level diagnostic characters used by Stara et al. (2018), such as the shape and arrangement of certain plates that compose the plastron of the oral face, are primarily used. The Sardinian spatangids are compared with both fossil species (from European and peri-mediterranean locations) and extant species (distributed worldwide).

Morphometric measurements and genetic analyses are used in combination for the first time to complement and support the results of the structural–morphological analyses.

The diagnostic characters, useful to distinguish the different forms under study (genera and/or species), are fully described and discussed. The new data can help in addressing taxonomic ambiguities within echinoids, as well as in improving species identification, and hence biodiversity assessments in the Mediterranean region.

2 Material and methods

2.1 Sampling

The study was primarily based on the analysis of 270 recent spatangids, trawled along the coasts of Sardinia during the experimental Mediterranean International Trawl Surveys (MEDITS; Spedicato et al., 2019) from 2018 to 2019 or available in museum collections (Figure 1 and Table 1). A subset of 21 specimens was preserved in alcohol for the genetic analyses, while the others were preserved as dried tests and were mostly deprived of spines.

To compare the oral schemes of the Sardinian samples and other extant species, fossils of Spatangidae of sedimentary rocks from the Oligocene to Pleistocene were studied from 1) Europe (Germany, Ukraine, and Italy), 2) North Africa (Melilla, Spain), and 3) USA (Florida). Other data, used for comparison in morphometric analyses or the plating reconstruction, were taken from bibliographic or museum sources (Table 1).

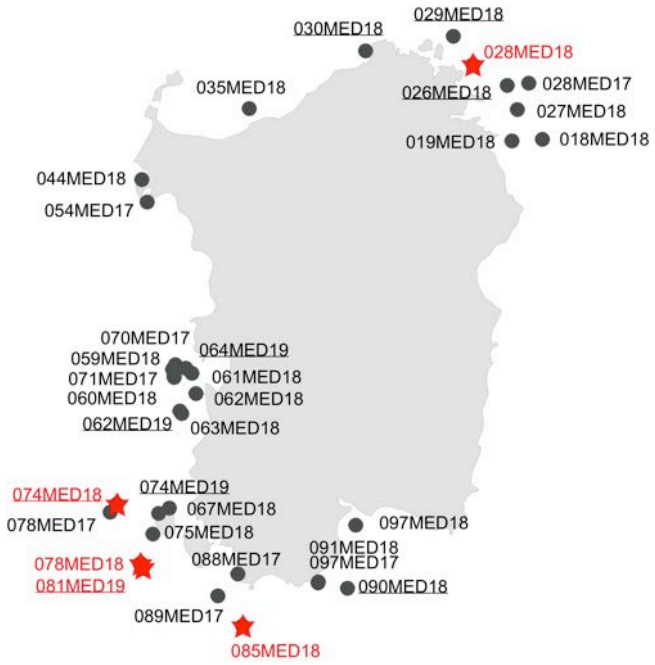

FIGURE 1
Map of the site collection during the MEDITS trawling campaign carried out along the Sardinian coasts. Circles in black = morphotype A (*Spatangus purpureus*); same red = morphotype B (*Propespatagus* sp. 1).

10.3389/fmars.2023.1033710

TABLE 1 Summary information on the spatangids analyzed.

Species	Institution	Acronym	Recent or fossil	Locality	N	Notes	Reference
Spatangus purpureus	Università degli studi di Cagliari, Italia	UNICA	Recent	Sardinia (Western Mediterranean)	230	Morphotype A	Present study
S. purpureus	Museo Aquilegia Masullas, Italia	MAC	Recent	Sardinia (Western Mediterranean)	30	Morphotype A	Present study
***Propespatagus* sp. 1**	Università degli studi di Cagliari	UNICA	Recent	Sardinia (Western Mediterranean)	9	Morphotype B	Present study
***Propespatagus* sp. 1**	Museo Aquilegia Masullas, Italia	MAC	Recent	Sardinia (Western Mediterranean)	1	Morphotype B	Present study
Spatangus* cf. *purpureus	Museo Aquilegia Masullas, Italia	MAC	Fossil	Pliocene Otranto, Puglia, Italy	1	MAC PL.2015 Pliocene	Present study
Spatangus* cf. *purpureus	Museo Aquilegia Masullas, Italia	MAC	Fossil	Terre Rosse, Siena Tuscany, Italy	1	MAC PL.2016 Pliocene	Present study
Spatangus* cf. *purpureus	Museo Aquilegia Masullas, Italia	MAC	Fossil	Ostia, Latium, Italy	1	MAC PL.2017 Pleistocene, Holocene	Present study
Spatangidae ind.	Museo Aquilegia Masullas, Italia	MAC	Fossil	Chesapeake Bay, Florida, USA	1	Cas.003, Caschili Collection Mio-Pliocene	Present study
S.* cf. *purpureus	Museo Aquilegia Masullas, Italia	MAC	Fossil	Otranto, Puglia,	1	F. Ciapelli Collection, Prato, Italy, Pliocene nn	Present study
***Propespatagus* sp.**	Museo Aquilegia Masullas, Italia	CIA.C MAC	Fossi	Otranto, Puglia,	2	F. Ciapelli Collection, Prato, Italy, Pliocene. classified as *Granopatagus* sp.nn	Present study
Sardospatangus caschilii	Museo Aquilegia Masullas, Italia	MAC	Fossil	Isili, Cagliari province, Sardinia	7	Miocene, Burdigalian, PL.344; 1551–1556	Stara et al., 2018
***Propespatagus* sp. 1**	Donné d'Observations pour la Reconnaissance et l'Identification de la faune et la flore Subaquatiques	DORIS	Recent	France, N–W Mediterranean	1	Classified as *Spatangus subinermis*	https://doris.ffessm.fr. n 1253 Foto Frèdéric CHEREAU
Propespatagus* cf. *subinermis	Museo paleontologico il Mare Antico Salsomaggiore Terme	MUMAB	Fossil	Plio-Pleistocene Rio Stirone, Parma	2	Coll. E. Borghi Moden, as *Granopatagus subinermis.* nn	Néraudeau et al., 1998
Propespatagus* cf. *subinermis	Museo paleontologico il Mare Antico Salsomaggiore Terme	MUMAB	Fossil	Plio-Pleistocene Rio Stirone, Parma	1	Coll. E. Borghi Modena, as *G. subinermis.* nn	Néraudeau et al., 1998
Spatangus* cf. *purpureus	Museo paleontologico il Mare Antico Salsomaggiore Terme	MUMAB	Fossil	Plio-Pleistocene Rio Stirone, Parma	1	Coll. E. Borghi Modena nn	Néraudeau et al., 1998
Spatangus inermis Mortensen (1913)	Stazione Zoologica Anton Dorn, Naples, Italy	SZN	Recent	Ischia, gulf of Naples	2	Holotype no. 1097 and 1 Paratype number	Mortensen, 1913

(Continued)

TABLE 1 Continued

Species	Institution	Acronym	Recent or fossil	Locality	N	Notes	Reference
***Spatangus* sp2**	Natural History Museum of Vienna, Geological— Paleontological Department, Austria	NHMW	Fossil	Badenian (Miocene) of Podjarków, bei Kurovice, Ukraine	1	(Sptangus desmaresti) No. 1859.0045.556	Kroh (2005)
***Spatangus desmaresti* Goldfuss, 1829**	Museum d'Histoire Naturelle, Genève, Suisse	MHNG	Fossil	Doberg, Westphalia, Germany.	1	de Loriol collection no. 127-27828	Smith and Kroh, 2011
***Spatangus saheliensis* Pomel, 1887**	Muséum National d'Histoire Naturelle, Paris, France	MNHNF	Fossil	Miocene-Pliocene of Melilla, Spain	1	Coll. Lachkhem no. R62132	Lachkhem and Roman, 1995
***Spatangus californicus* H.L. Clarck**	Muséum National d'Histoire Naturelle, Paris, France	MNHNF	Recent	S. Catalina Island, California, USA Japan	2	A66829 L23322 Stored as *Spatangus luetckeni*	Present study Mortensen, 1951
***Spatangus luetckeni* A, Agassiz, 1872**	–	–	Recent	Hokodate, Japan	1	–	Schultz, 2009, in Kroh and Mooi, 2022
***Propespatagus paucituberculatus* (A. Agassiz & H.L. Clarck, 1902)**	Museum of Comparative Zoologiy at Harvard.	MCZ Harvard	Recent	Hawaiian Islands	1	Plate III	Mortensen, 1951
***Propespatagus multispinus* (Mortensen, 1925)**	Copenaghen Museum Museum of New Zealand	NHMD	Recent	Aukland-Campbell Island New Zealand	2	Cotype Plate II Type n ECH.82	Mortensen, 1951 Collections.tepapa.govt.nz
***Propespatagus capensis* (Döderlein, 1905)**	–	–	Recent	East London S. Africa	1	Plate I	Mortensen, 1951
***Propespatagus raschi* (Lovén, 1896)**	The Swedish Museum of Natural History	SMNH	Recent	Shetland Islands North Atlantic	2	Plate XIII PlateII	Lovén, 1896 Mortensen, 1951
***S. californicus* H.L. Clarck**	–	–	Recent	Baja California, Mexico	1	Plate II	Mortensen, 1951
***Spatangus mathesoni*, McKnight, 1967**	National Institute of Water & Atmospheric Research	NIWA	Recent	New Zealand	2	Paratype P-42 and no. 50049	Present study
***Plethotaenia spatangoides* (A. Agassiz, 1883)**	–	–	Recent	Cuba	1	Plate 39, Figures 1–10	Mortensen, 1951.
***Plethotaenia angularis* Chesher, 1968**	–	–	Recent	Bahama to Barbados, Caribbean	1		Chesher, 1968;Schultz, 2009, in Kroh and Mooi, 2022
***P. angularis* Chesher, 1968**	Smithsonian Institution	NMNH	Recent	Caribbean	1	E10726,	Chesher, 1968;Smith and Kroh, 2011

The institution is responsible for the sampling or the possession of museum collections and related acronyms, the locality of the collection, and the number of specimens, notes, and references. In the first column, the species name corresponds to the new denomination proposed in this study.

2.2 Structural, morphological, and biometric analyses

The biometric measurements taken from the samples analyzed in this work are illustrated in Figures 2A, B. The abbreviations used are those commonly used in specialist literature.

TL = length of the test; TW = width of the test; TH = height of the test; α = angle of divergence between the anterior paired petals; β = angle of divergence between the posterior paired petals; L1 = height of the periproct, detected along the interradial sutures; L2 = width of the periproct, at the widest point, as shown in Figure 2A; L3 = distance between the lower edge of the periproct and the support base of the test; L4 and L5, length and width of the anterior paired petals, respectively; L6 and L7, length and width of the posterior paired petals, respectively; L8 = distance between the frontal genital pores and the posterior margin of the test; L9 = depth of the sinus anterior to the ambitus; L10 = distance between the most advanced point of the front "shoulders" of the test; L11 = distance between the anterior margin of the labrum and the anterior margin of the test; L12 = length of the labrum L13 = length of the sternal plates; L14 = width at the basis of the labrum; L15 = width of the group of plates formed by the sternals and those belonging to the adjacent ambulacra I and V; L16 = maximum width of the sternal plates; L17; distance between the two outermost points, in transverse section, of the sub-anal fasciole; FW = fasciole width (thickness).

Measurements of TL, TH, and TW were performed using a caliper measuring to one-twentieth of a millimeter; TL was reported in mm, while the other measurements were reported in % of TL; the length and

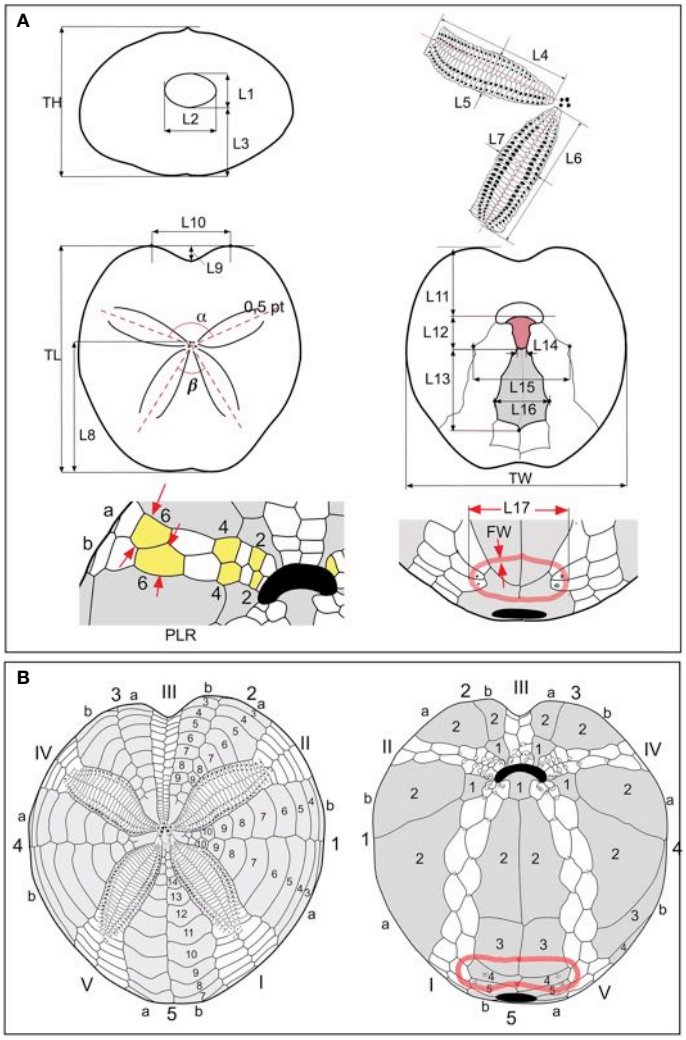

FIGURE 2
(A) Scheme of biometric measurements used in this study. **(B)** Conventional numbering of plates according to Lovén (1874). The ambulacral plates are numbered in Roman numerals; the interambulacral in Arabic numerals. Each area is divided into two columns "a" and "b"; the count occurs counterclockwise in the aboral view and clockwise in the oral view.

width of the front petal (L4 and L5) were measured by a caliper in mm and then converted into % of TL; the same for the measurements concerning the periproct (L1, L2, and L3); the measurement of L1 was taken between the opening point of the periproct along the interradial suture of interambulacrum 5; the other measurements were taken from the photos, as detailed below; the angles are reported in degrees. To obtain these measurements, each specimen included in the database was photographed by a Nikon D 300s camera, equipped with a Zeiss Macro-Planar 2/50 mm lens, in order to minimize distortions. Adoral, posterior, and anterior photographs were taken with the camera perpendicular to the interested faces. Each view is the result of many photos combined using the Helicon Focus program, version 4.2.9, d-STUDIO for Mac OS X, in order to optimize the final depth of field. The other morphometric characters were determined directly in % of TL, from the photos analyzed in the Autodesk Graphic 3.1 program, for Mac.

In addition to the specimens caught in Sardinian seas, the morphological analyses included a further 39 specimens (Table 1) in four genera: *Sardospatangus* Stara, Charbonnier et Borghi, 2018 (†); *Spatangus* Gray, 1825; *Pletothaenia* Clark, 1917; and *Granopatagus* Lambert, 1915.

With the use of a similarity matrix based on the Euclidean distance, multivariate differences in the morphological measurements of the different samples were illustrated by the Canonical Analysis of Principal Coordinates (CAP; Anderson and Willis, 2003), obtained using the PRIMER v7 software. The Primer V7 software also used to verify the statistical significance of the differences between the groups identified by the CAP, through the analysis of similarities (ANOSIM) test, and to identify which measurements contributed to these differences, by means of the SIMPER test (SIMilarity PERcentages) (Clarke and Gorley, 2015).

The test plating in oral and aboral views of all the species analyzed in this work was drawn following Lovén (1874) (Figure 2B).

Boxplots (Figure S2), with interpolation of the quartiles, were obtained using the software PAST 3.11, Paleontological Statistics software package for education (Hammer et al., 2001).

2.3 DNA extraction, amplification, sequencing, and alignment

A subset of the specimens analyzed morphologically were investigated using molecular tools. Genomic DNA was extracted using a PureLink® Genomic DNA Kit, based on the selective binding of DNA to a silica-based membrane, according to the manufacturer's protocol. The genomic DNA was eluted in 50 µl of Elution Buffer (10 mM of Tris-HCl).

Two genes were selected for analysis: the mitochondrial 16S rRNA (16S) and cytochrome *c* oxidase subunit1 (COI). Polymerase chain reaction (PCR) amplification of fragments was performed with 25-µl reaction volume. Each reaction tube contained 3.5 µl of 10× buffer (Dream Taq® buffer, Thermo Fisher Scientific, Waltham, MA, USA), 2.5 µl of 2 mm dNTPs, 0.2 µl of each 20 mm primer, 0.16 µl of Taq polymerase (Dream Taq® Thermo Fisher Scientific), and 2.5 µl of DNA (50–100 ng). COI fragment was amplified using the primer pair EchinoF1 (5′-TTTCAACTAATCATAAGGACATTGG-3′) and EchinoR1 (5′-CTTCAGGGTGTCCAAAAAATCA-3′) (Ward et al., 2008). PCRs started with denaturation at 95°C (5 min) and were followed by 95°C (30 s), 50°C (60 s), and 72°C (60 s) for 35 cycles. The 16S fragment was amplified using the primer pair 16 Sar (5′-CGCC TGTTTATCAAAAACAT-3′) and 16Sbr (5′-CCGGTCTGAAC TCAGATCACGT-3′) (Palumbi et al., 1991). PCR conditions used were denaturation at 94°C (2 min) followed by 94°C (25 s), 47°C (60 s), and 72°C (60 s) for 40 cycles. The PCR products were checked on an agarose gel (1.5%) with SYBR® Safe DNA Gel Stain (10,000×). Purification and sequencing were carried out by Macrogen Europe (Amsterdam, The Netherlands). Alignments were elaborated using the ClustalW method (Thompson et al., 1994) implemented in MEGA v7 (Kumar et al., 2016).

2.4 Genetic analyses and phylogenetic reconstructions

Since the partition homogeneity test implemented in PAUP* v4.0a169 (Swofford, 2003) indicated that the 16S and the COI datasets did not significantly differ in their phylogenetic signal ($p = 0.53$), the two mtDNA markers were analyzed separately and concatenated. The principal indices of genetic diversity (the number of haplotypes [H], haplotype diversity [hd], nucleotide diversity [π] and relative standard deviations, and the average number of nucleotide differences [k]) were estimated in DnaSP, while the p-distance among sequences and between the two *Spatangus* morphotypes were performed in MEGA. In order to evaluate the relationship among the sequences from Sardinian specimens and the homologous sequences deposited for the genus *Spatangus* in GenBank and BOLD public databases, PAUP and MrBayes v3.2.6 (Ronquist et al., 2012) software were also used for the phylogenetic reconstruction. Specifically, four different methods were used to investigate the phylogeny: the neighbor joining (NJ), the maximum parsimony (MP), and the maximum likelihood (ML), performed in PAUP with 1,000 bootstrap replicates, and the Bayesian inference (BI) method obtained using MrBayes with 20 million generations and 25% of burn-in. In the phylogenetic reconstructions, sequences of *Echinocardium laevigaster* A. Agassiz, 1869 (COI: AJ639913; 16S: AJ639813; Stockley et al., 2005) and *Brissus unicolor* (Leske, 1778) (COI: MN683889-91 (Collin et al., 2020); 16S: AJ639822, Stockley et al., unpublished) were used as the outgroup.

The molecular data were also combined into a matrix of 38 morphological characters, since the use of independently evolving characters together may best represent the evolution of the species and improve the accuracy of phylogenetic reconstructions (Chippindale and Wiens, 1994; Huelsenbeck et al., 1996; Bucklin and Frost, 2009). The matrix considers only the 38 characters that can be better applied to spatangids than that by Stockley et al. (2005) and Kroh and Smith (2010), which include 88 characters. The full list of morpho-structural characters and character state definitions used in phylogenetic reconstructions are listed in the Supplementary Material and Table S1.

The combined morphological/molecular dataset was statistically evaluated for incongruence using the partition homogeneity test, and the phylogenetic trees were reconstructed using the same approaches and the same software described for the molecular analysis: weight = 5 and 1 for morphological and molecular characters, respectively, as described in Bucklin and Frost (2009). The same methods were applied using only the morphological character matrix, but in this case, all characters were unordered and unweighted.

3 Results

3.1 Morphology–morphometrics

Considering the whole sample of spatangids collected in Sardinian seas, two different morphotypes were found: the vast majority of specimens (n = 260) corresponded to m orphotype A, i.e., the commonest Mediterranean species S. purpureus, while 10 specimens, provisionally referred to here as morphotype B, showed a similar general shape to morphotype A but a different plastron plating. The observations made on the specimens collected in Sardinian seas are summarized in Table 2. The test size (TL) ranges from 64.5 to 123 mm, but with the largest frequency of medium-large individuals, from 93 to 110 mm. The sample showed a wide variability of the main measurements, but some characters have a lower variability (low SD).

CAP analysis based on a similarity matrix of the Euclidean distances clearly identified two groups (Figure 3) (ANOSIM $p < 0.05$). The SIMPER test (Table S2) highlighted the contribution of the 10 variables in the differentiation of the two morphotypes. The top five variables that provided the greatest contribution to the differentiation in decreasing order are L17 (16.93%), L4 (9.76%), L3 (6.74%), L16 (6.73%), and L6 (6.58%). The difference between morphotypes A and B is clearly visually highlighted in the boxplot of Figure S2 based on L17 and FW measurements.

Considering the plating (Figures 2A, B, 4A, B), the main differences between the two forms were found in the following: 1) the fasciole pathway, which is broad and surrounds two lobes (bilobed) on the episternal plates in morphotype A (mean L17 = 41.67), which is small and surrounds only one lobe (monolobed) in the center between the two episternals in morphotype B (mean L17 = 26.73); 2) ambulacral plates I.6.a, I.7.a, and I.8.a and V.6.b, V.7.b, and V.8.b (see Figure 2B) narrow and protrude toward the center

10.3389/fmars.2023.1033710

TABLE 2 Morphometric measurements in recent spatangids.

Measure	Overall				Morphotype A				Morphotype B			
	Min	Max	Mean	SD	Min	Max	Mean	Stand. dev.	Min	Max	Mean	SD
TL	64.50	123.50	123.50	13.98	64.50	123.50	101.67	14.26	96.70	122.70	106	8.37
TW	81.00	102.30	102.30	2.95	81.00	102.30	94.48	2.96	89.70	97.60	92.94	2.44
TH	**45.00**	**60.70**	**60.70**	**2.97**	**46.50**	**60.70**	**53.48**	**2.86**	**45.00**	**54.70**	**51.14**	**3.79**
FW	0.70	3.60	3.60	0.56	0.70	1.90	1.21	0.27	3.00	3.60	3.32	0.21
L1	6.90	19.80	19.80	1.73	6.90	19.80	19.80	1.74	7.60	9.10	9.10	0.43
L2	9.00	20.20	20.20	1.49	9.00	20.20	20.20	1.43	10.96	12.50	12.50	0.60
L3	**9.48**	**27.20**	**27.20**	**3.18**	**11.30**	**27.20**	**27.20**	**2.90**	**9.48**	**26.50**	**26.50**	**6.63**
L4	**29.60**	**49.50**	**49.50**	**3.25**	**34.80**	**49.50**	**41.98**	**2.58**	**29.60**	**36.60**	**33.32**	**2.10**
L5	8.70	18.30	18.30	1.55	10.00	18.30	18.30	1.39	8.70	11.30	11.30	0.94
L6	**32.30**	**47.20**	**47.20**	**2.74**	**36.40**	**47.20**	**41.53**	**2.39**	**32.30**	**38.50**	**35.75**	**2.31**
L7	8.50	17.80	17.80	1.51	9.30	17.80	17.80	1.37	8.50	11.60	11.60	0.96
L8	**41.40**	**65.40**	**65.40**	**2.82**	**41.40**	**65.40**	**65.40**	**2.80**	**57.60**	**63.60**	**63.60**	**2.36**
L9	**4.10**	**11.90**	**11.90**	**1.40**	**4.10**	**7.90**	**5.86**	**0.74**	**9.30**	**11.90**	**10.71**	**0.98**
L10	**14.90**	**29.30**	**29.30**	**2.09**	**18.00**	**29.30**	**22.35**	**1.78**	**14.90**	**21.50**	**17.88**	**2.15**
L11	19.90	31.20	31.20	2.20	19.90	31.20	31.20	2.15	20.60	25.50	25.50	1.69
L12	5.30	14.10	14.10	1.44	5.30	14.10	14.10	1.30	5.60	7.10	7.10	0.59
L13	34.00	44.80	44.80	1.75	34.00	44.80	44.80	1.77	36.00	41.30	41.30	1.44
L14	3.40	11.00	11.00	1.57	3.90	11.00	11.00	1.50	3.40	5.40	5.40	0.85
L15	**29.30**	**47.30**	**47.30**	**2.74**	**29.30**	**47.30**	**47.30**	**2.61**	**32.00**	**37.10**	**37.10**	**1.66**
L16	**22.60**	**37.20**	**37.20**	**2.75**	**24.20**	**37.20**	**37.20**	**2.39**	**22.60**	**26.70**	**26.70**	**1.37**
L17	**25.40**	**48.90**	**48.90**	**4.06**	**36.70**	**48.90**	**41.67**	**2.09**	**25.40**	**27.80**	**26.73**	**0.81**

Acronyms of the measurements are described in the main text and SM. TL is reported in mm, and the other measurements are given as % of TL. The measurements in bold are indicated by the SIMPER test as those contributing to the differentiation between morphotype A and B. Minimum, maximum, and mean values ± standard deviation (SD) are shown for the whole sample and morphotype A/B separately.

of the fasciole occluding (or almost) interambulacrum 5 in morphotype B; 3) the episternal plates' shapes are broad and not very indented by the adjacent ambulacra in morphotype A, while they are narrow, long, and deeply indented by the ambulacral plates in morphotype B.

Furthermore, morphotype B has a narrow and deep anterior sinus, while it is wide and shallow in morphotype A (L9 = 10.71 and 5.86, respectively).

After verification of the number of ambulacral plates in contact with the labrum, no variability was found in the ratio of labrum/number of adjacent ambulacral plates, but growth anomalies only. Of the specimens, 7.69% had labrum deformations, and only 4.23% had at least two plates on one side of the labrum. Other data are summarized in Table S3 and Figures S3, S4.

Concerning the number of primary tubercles (or their presence/absence) in certain interambulacral aboral areas, we observed that their number is very variable but also that they are present in all five interambulacra of all the individuals studied. Moreover, we also observed that these tubercles are always present in the five interambulacra but in a constantly lower number in morphotype B specimens.

3.2 Morphological and morpho-structural comparisons

Both recent and fossil spatangids were compared to morphotypes A and B, examining plating and morpho-structural matrix characters.

Firstly, the schemes (plating) of the oral face of morphotype A and morphotype B were compared with species classified as *Spatangus*. *Spatangus inermis* Mortensen (1913), *Spatangus paucituberculatus* (A. Agassiz & H.L. Clark, 1902), *Spatangus multispinus* (Mortensen, 1925), *Spatangus raschi* Mortensen (Lovén, 1869), and *Spatangus capensis* Döderlein (1905) showed the same scheme as morphotype B (Figure 5, in order: 5b, c, d, e, f). Instead, *Spatangus luetkeni* A. Agassiz, 1872, *Spatangus californicus* Clark, 1917, and *Spatangus mathesoni* McKnight, 1967 have intermediate characters between the two morphotypes under examination.

Furthermore, the study of fossil species (listed in Table 1) highlighted that *G. subinermis* Pomel, 1875 (Figure 5A) had many features in common with morphotype B. *Spatangus desmaresti* (Figure 6C) had the same basic structure as the plastron of morphotype A (Figure 4A). Instead, *Sardospatangus caschilii* and *Sardospatangus saheliensis* (Figures 6A, B) have peculiar plating,

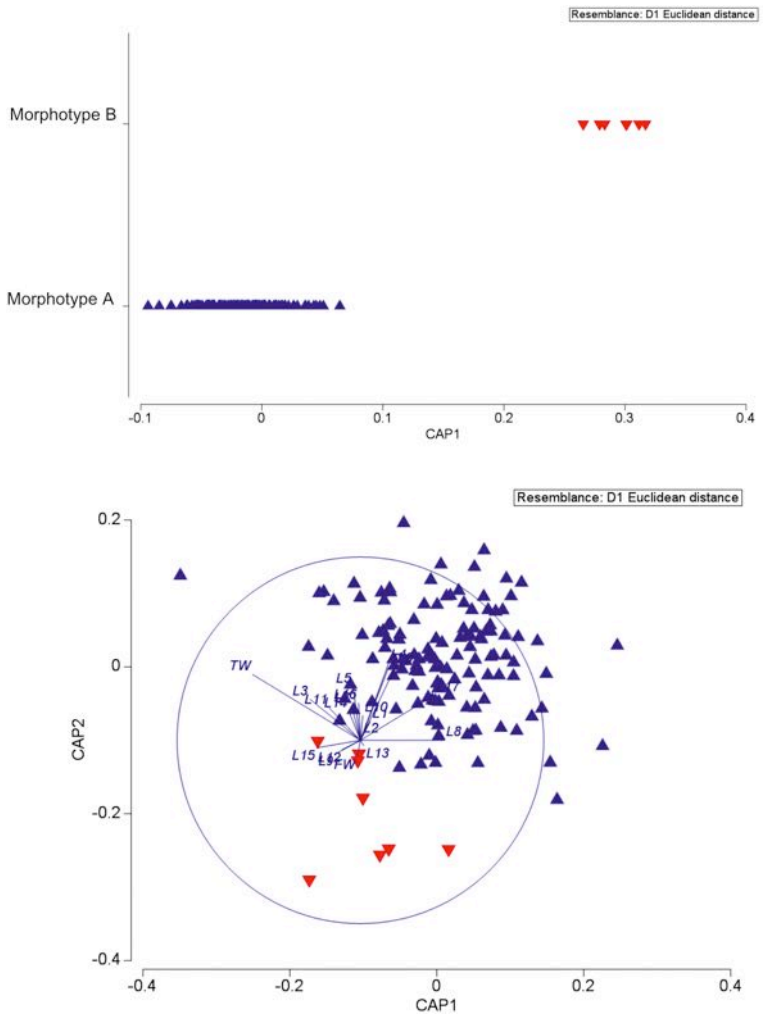

FIGURE 3
Canonical analysis of principal coordinates of biometric data of the two spatangids under study.

different from both morphotypes A and B. *Sa. saheliensis*, which has a very deep groove, small petals (Figure 6B), and few primary tubercles, differs from *Sa. caschilii*, which has a shallow groove and large petals (Figure 6A). At the genus level, however, we can see that *S. paucituberculatus* (Figure 5C), despite its very deep groove, relatively small petals, and rare primary tubercles (as *Sa. saheliensis*), falls into another genus due to the different plastron structure.

S. subinermis (Figure 5A) is superimposable, in terms of the structure of the plastron and length of petals, to the extant morphotype B (Figure 4B); the extant *S. purpureus* (morphotype A) (Figure 4A) has the same basic shape of the plastron (a single ambulacral plate on each side of the labrum and a wide and bilobed fasciole, with wide and not indented episternals) of *S. desmaresti* (Figure 6C). Moreover, *Spatangus* sp. 1 of the Miocene of Ukraine (Figure S5) shows the labrum with only one plate per side of large episternal plates (even if the fasciole is not visible). Finally, also *Spatangus* cf. *purpureus* of the Pleistocene of Italy (Figure S6) share all the characters of the extant *S. purpureus*.

The extant *Plethotaenia angularis* (Figure 6D) shares with morphotype B the main characters of the plastron including the shape of the subanal fasciole, but the presence of pseudofasciole around the petals on the aboral face (Figure 6D up) clearly detaches it from the latter, as, however, it detaches from *Sardospatangus* (fossils) and *Spatangus* (extant and fossils), which have a wide and bilobed fasciole (cf. Figures 6A down, b down; 4A down).

Finally, *S. californicus* (Figure 6E) and *S. mathesoni* (Figure 6F) can be distinguished from all other forms. They first differ in having a wide fasciole (apparently monolobate) and the episternal plates intermediate between those of morphotype A and morphotype B; the latter shows small petals and plastron superimposable to that of morphotype B (Figure 4B with Figures 6E, F), while the anterior sinus is deep and narrow, and the test is low and vaguely discoid (in adult individuals) as in *Plethotaenia* (Figure 6F); the fossil spatangid from the Florida Mio-Pliocene (USA) is very similar to *S. purpureus*, except for the fasciole, which is small and (apparently) monolobed (Figure S7A, B).

3.3 Phylogenetic analyses using molecular and morphological data

To shed light on morphological differences recorded among specimens of spatangoids collected in Sardinian waters in 2018 and

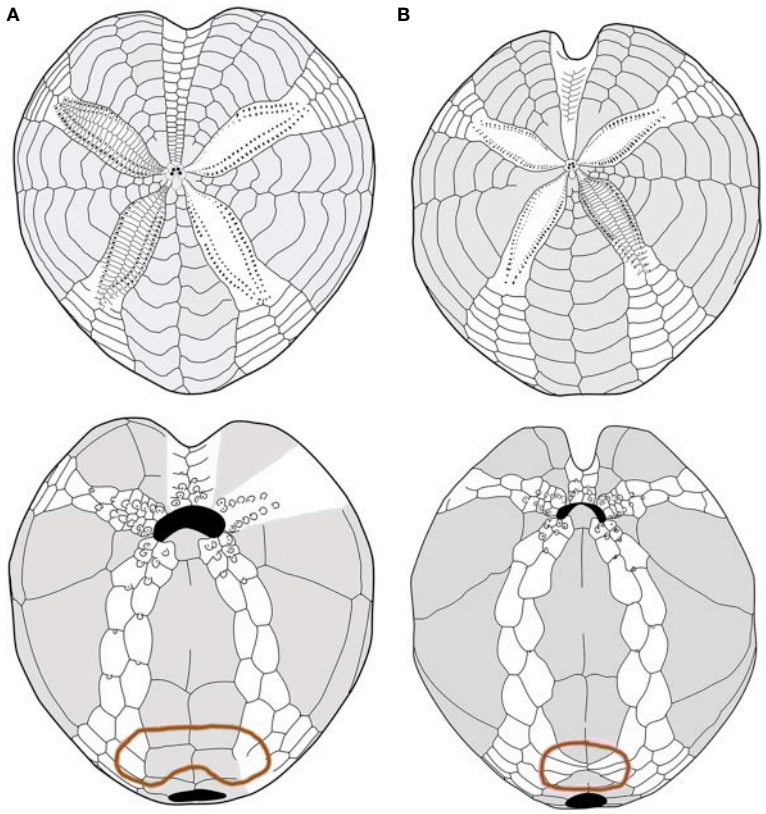

FIGURE 4
(A, B) Comparison between schemes (or pattern): **(A)** *Spatangus purpureus*, aboral (up) and oral view; **(B)** *propespatagus* sp. 1 aboral (up) and oral view.

2019 and to investigate the taxonomical relationships between morphotypes A and B, 16 and 5 specimens form morphotypes A and B, respectively, were investigated using molecular tools.

All specimens were successfully processed for DNA extraction, but some individuals failed to provide PCR products for one or several fragments. A total of 15 individuals were successfully sequenced for one or both markers: 10 individuals for morphotype A and 5 for morphotype B (details of the specimens are provided in Table S4). A final alignment of 646 and 522 bp was obtained for the COI and 16S fragments, respectively. The principal indices of genetic diversity are reported in Table 3. The Sardinian individuals are characterized by a high haplotype diversity (hed_{COI} = 0.857; hd_{16S} = 0.769; hd_{conc} = 0.923) and a low nucleotide diversity (π_{COI} = 0.027; π_{16S} = 0.014; hd_{conc} = 0.022) for both the markers, while the average number of nucleotide differences results higher for concatenated markers (k = 25.87) and COI (k = 17.55) than for the 16S marker (k = 7.36). Morphotype A showed a higher number of haplotypes than B, which showed only one substitution for COI and no variable sites for the 16S (Table 3).

Concerning the genetic distances between the two morphotypes, pairwise DNA differences ranged between 33 and 37 for COI and between 13 and 15 for 16S. The p-distances between groups were 5.3% and 2.7% for COI and 16S, respectively. The concatenated markers showed a genetic differentiation that ranged between 47 and 52 nucleotides, corresponding to a p-distance of 4.2%.

The Sardinian samples were compared with homologous sequences from the public repositories; a total of 14 sequences for COI (final alignment: 560 bp), 10 sequences for 16S (final alignment: 422 bp), and 3 concatenated sequences (final alignment: 1,108 bp) were added to our alignments (see Table S5 for details).

In all the trees, with the four methods used for both separate and concatenated DNA markers (Figures 7, S8, S9), the Sardinian sequences clustered in two different groups with high statistical support, corresponding to morphotypes A and B. Sequences from morphotype A clustered with the sequences deposited in GenBank as *S. purpureus* (O.F. Muller, 1776), while sequences from morphotype B, which were separated from morphotype A sequences, are placed in a clade with other species (e.g., *S. californicus* H. L. Clark, 1917, *S. multispinus* Mortensen, 1925, and *S. raschi* Lovén, 1869). The closest sequences to morphotype B are those deposited as *S. raschi*. The same findings were obtained also for the trees of combined morphological and molecular characters (Figure 8), confirming the occurrence of two clearly separate groups in the Sardinian waters. Once again, the individuals from morphotype A are attributed to the species *S. purpureus*, while specimens from group B seem different from the currently described species of Spatangidae but are placed together with the species *S. multispinus* and *S. raschi*.

The analysis of the trees obtained from the morphological character matrix (Figure S10) showed several groups within the clade of the family Spatangidae. In particular, once more, the species *S. purpureus*, corresponding to our morphotype A, is placed in a separate clade of the individuals belonging to morphotype B, supporting the differentiation identified from the molecular tool.

Finally, Figure S11 shows the stratigraphic relationship between fossils species analyzed.

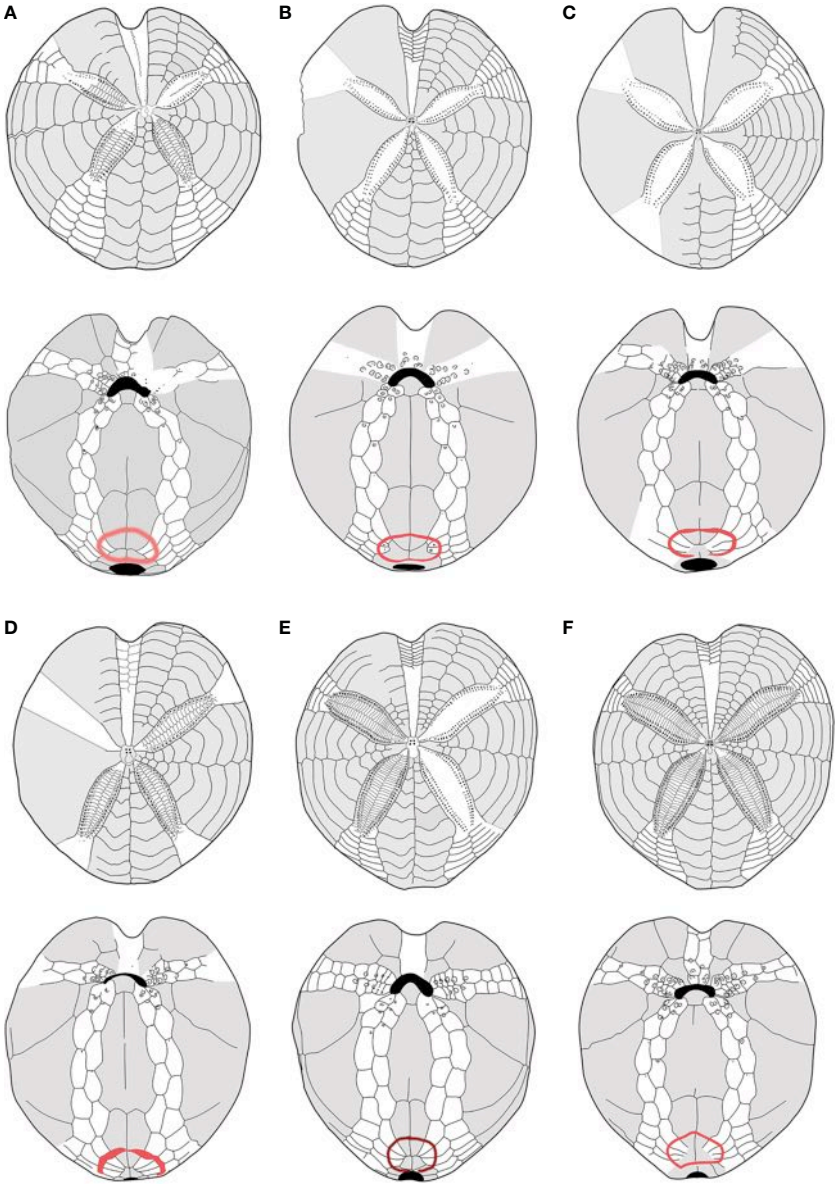

FIGURE 5
(A–F) Structural similarities in aboral (up) oral and oral (down) schemes, between recent and fossil species of *Propespatagus* analyzed in this work: **(A)** *Propespatagus subinermis*, Pliocene di Otranto, Lecce, Puglia (Italy); **(B)** *Propespatagus inermis*, Gulf of Naples, Mediterranean (redrawn from Mortensen, 1913); **(C)** *Propespatagus paucituberculatus*; **(D)** *Propespatagus multispinus*; **(E)** *Propespatagus raschi*, Shetland Islands; **(F)** *Propespatagus capensis*, seas of Cape Town, South Africa. Schemes (platings) c– f were redrawn from Mortensen (1951).

In summary, based on morphological and genetic results for morphotype B, we establish a new genus, named *Propespatagus* gen. nov., where morphotype B specimens are to be hosted. See section 5 for the formal description.

4 Discussion

This article aims to contribute to improving the knowledge of the diversity, distribution, and systematics of the Spatangidae in the Mediterranean Sea, through the study of specimens recently collected in the Western Mediterranean (Sardinia), using, for the first time, a combined approach based on morphometric measurements and genetic and structural–morphological analyses. Furthermore, paleontological data are used to complement the data and support the results of the analyses.

Morphometrics, genetics, and structural morphology converge toward the occurrence of two distinct species in the area under investigation: morphotype A is easily identifiable as *S. purpureus*, and morphotype B largely corresponds to the description of *S. subinermis* (*sensu* Kroh and Mooi, 2022). The observations made on the specimens collected in Sardinian seas showed a wide variability of the main measurements and the difficulty in finding resolutive characters for the identification of taxa (Table 2), confirming what was observed by Bonnet (1926). For instance, focusing on the number of primary tubercles in certain interambulacral aboral areas cannot be regarded as clearly resolutive since we observed in our sample of *S. purpureus* (260 individuals) that, as claimed by Bonnet (1926), this

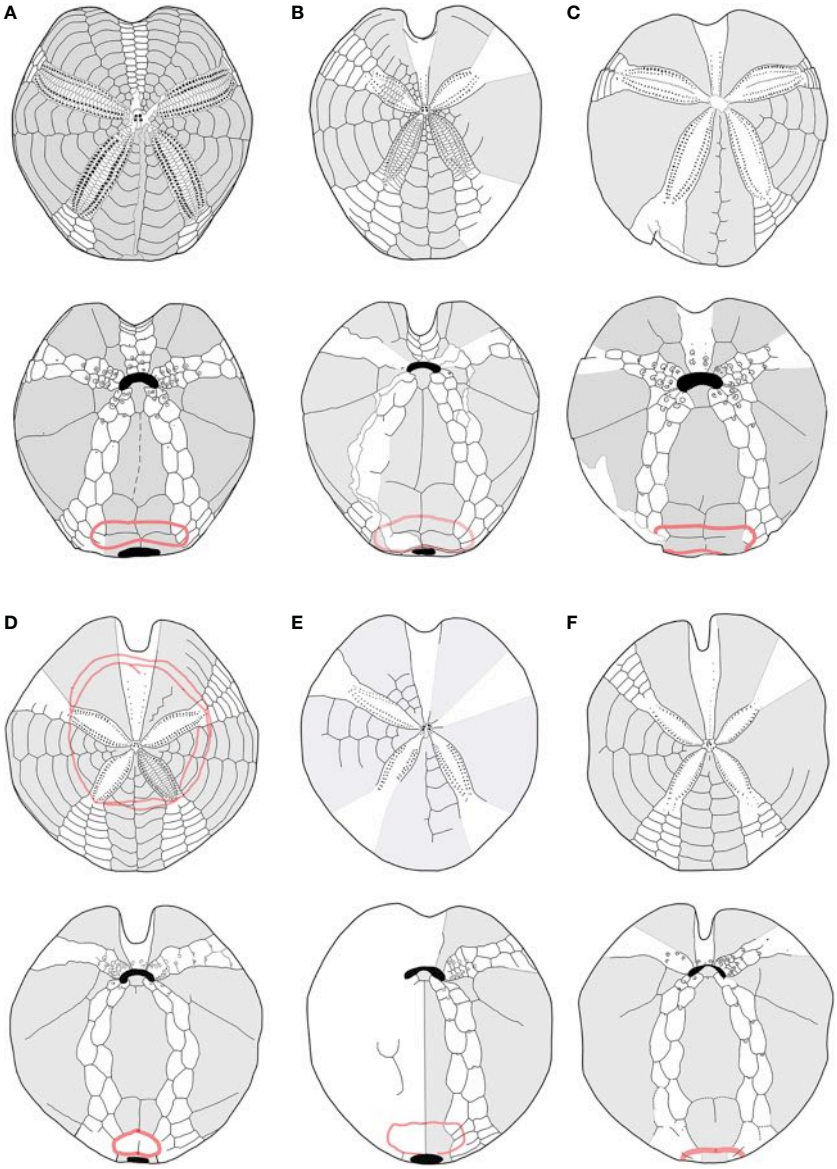

FIGURE 6
(A–F) Structural similarities in aboral (up) oral and oral (down) schemes, between fossil and recent species of Spatangidae analyzed in this work. **(A)** *Sardospatangus caschilii*, Miocene, Burdigalian of Isili, Sardinia, Italy (MAC PL 344); **(B)** *Sardospatangus saheliensis*, Messinian-Pliocene of Melilla, Spain, North African coasts (MNHN no. R62132); **(C)** *Spatangus desmaresti*, Oligocene, Chattian of Doberg, Westphalia, Germany (MHNG no. 127-27828); **(D)** *Plethotaenia angularis*, Recent, Caribbean Sea (Redrawn from Schultz, 2009, in Kroh and Mooi, 2022; **(E)** *Spatangus californicus*, Baia California, Mexico (Redrawn from Mortensen, 1951); **(F)** *Spatangus mathesoni*, New Zealand, Station D0231 (NIWA paratype P42).

character is very variable, with the primary tubercles present in all five interambulacra of all the individuals studied; at the same time, we also observed, in our sample of morphotype B (10 individuals), that these tubercles are always present in the five interambulacra, but in a lower number. However, other structural features of the plastron plating (Figures 4A, B; the fasciole pathway, the ambulacral plates (I.6.a, I.7.a, and I.8.a as well as V.6.b, V.7.b, and V.8.b), the episternal plates' shape, and the shape and depth of the anterior sinus) allowed to clearly distinguish the two forms. Similarly, in our study, both morphometrics and genetics clearly separated the two types.

Despite the fact that the great variability observed by Bonnet (1926) was also present in our sample, it did not prevent the use of various diagnostic characters, appropriately chosen, for the separation between species and genera in the same family.

In this study, we observe that the variability described by McNamara (1982; 1987; 1988; 1989) was not present in the abundant sample of extant spatangid collected in Sardinia, as already seen by Stara et al. (2018) on a large sample of fossil Spatangidae specimens collected in the sedimentary rocks of the Sardinian Miocene.

Based on the peculiar features of morphotype B, here, we establish a new genus, named *Propespatagus* gen. nov., and we name the extant specimens studied *Propespatagus* nov. sp. 1, awaiting to have more material for a formal specific institution according to International Code of Zoological Nomenclature (ICZN) rules.

At the same time, based on the plating of the oral face similar to morphotype B, a number of species thus far attributed to the genus *Spatangus* (i.e., *S. inermis*, *S. subinermis*, *S. paucituberculatus*,

TABLE 3 Indices of genetic diversity for the Sardinian specimens calculated for the two mitochondrial markers and for the concatenated sequences.

	N	H	hd ± SD	π ± SD	k
COI					
Morphotype A	9	4	0.750 ± 0.112	0.0019 ± 0.0006	1.22
Morphotype B	5	2	0.600 ± 0.175	0.0009 ± 0.0003	0.60
Total	14	6	0.857 ± 0.056	0.0272 ± 0.0045	17.55
16S					
Morphotype A	9	4	0.694 ± 0.147	0.0016 ± 0.0005	0.83
Morphotype B	5	1	–	–	–
Total	14	5	0.769 ± 0.076	0.0141 ± 0.0022	7.36
16S+COI					
Morphotype A	8	6	0.929 ± 0.084	0.0019 ± 0.0005	2.25
Morphotype B	5	2	0.600 ± 0.175	0.0005 ± 0.0002	0.60
Total	13	8	0.923 ± 0.050	0.0222 ± 0.0032	25.87

N = number of sequences; H = number of haplotypes, hd = haplotype diversity, π = nucleotide diversity and relative standard deviations (SD), and k = average number of nucleotide differences.

S. multispinus, *S. raschi*, *S. capensis*) are transferred to *Propespatagus* gen. nov.

S. luetkeni, from the Japanese coasts, *S. californicus*, from the Gulf of California, and *S. mathesoni*, from New Zealand, remain in the genus *Spatangus* because their oral patterns show intermediate characters between the two reference genera, or the data in our possession are not sufficient for an in-depth analysis.

Concerning the fossils, the generic attribution of *S. desmaresti* is confirmed, having the same basic structure as the plastron of *S. purpureus*; genus *Sardospatangus*, with the species *Sa. caschilii* and *Sa. saheliensis*, is a valid genus as its features are different from our types A and B. The form previously called *G. subinermis* Pomel, 1875, of the Italian Plio-Pleistocene, is here proposed to be renamed as *Propespatagus subinermis* Pomel (1875) sp.

The subdivision between genera was mainly based on diagnostic characters of the oral face that, among all the districts of the spatangoid dermaskeleton, are the ones where evolution has worked both for plate accretion and for plate addition (Smith, 2005), constituting the "plastron". We also focused on the subanal fasciole, whose characters were considered by Smith and Stockley (2005) to be highly informative and reliable from a phylogenetic point of view.

The division between species within the two resulting genera (*Spatangus* and *Propespatagus*) was made using the same criteria, as well as a number of other characters (in part borrowed from Stockley et al., 2005 and Kroh, 2020), but in this case, tested in their variability. Some uncertainties in the species attributions made in the past remain, and this is for at least two reasons: 1) the choice of poorly diagnosed characters and 2) the scarcity of the material used in the

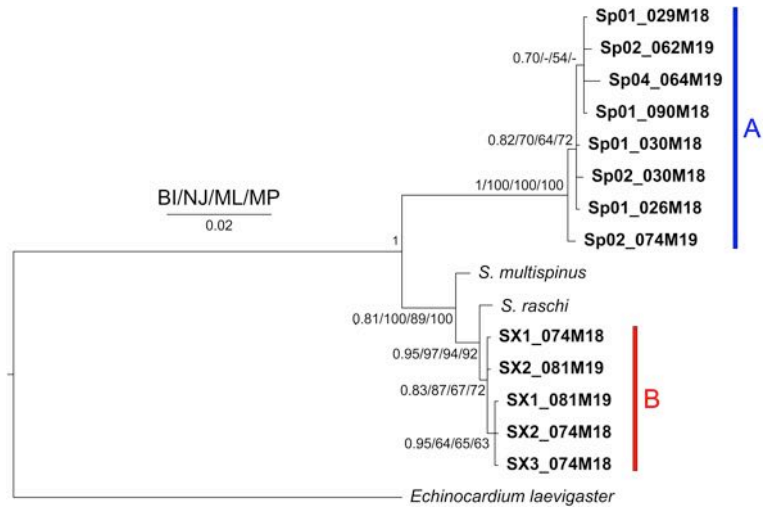

FIGURE 7
Tree obtained with the concatenated 16S and cytochrome c oxidase subunit1 (COI) sequences. Near the nodes are the values for the Bayesian probability (BI) or the bootstrap support (NJ/ML/MP). In bold are the Sardinian spatangids. The bars and capital letters A (blue) and B (red) indicate the sequences of morphotype A and B, respectively.

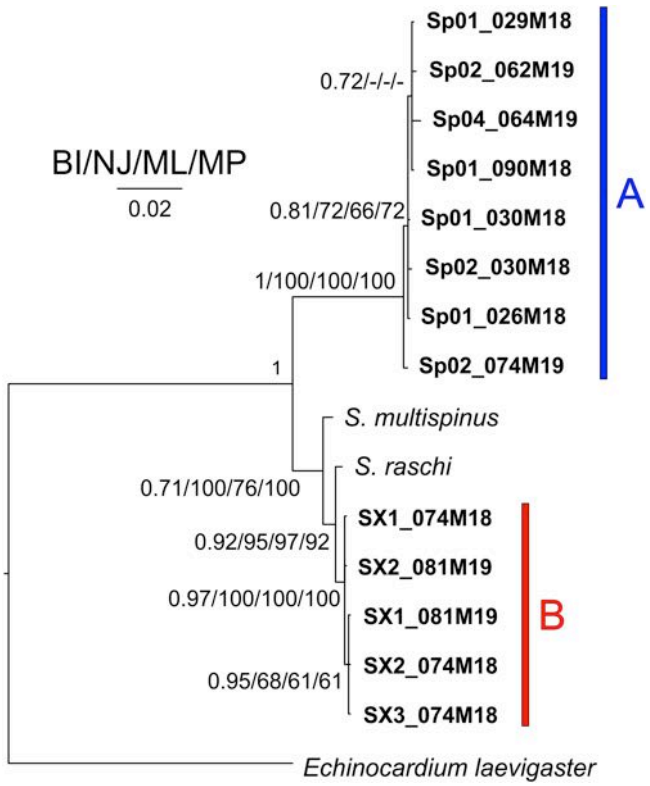

FIGURE 8
Tree obtained combining morphological and molecular characters. Near the nodes are the values for the Bayesian probability (BI) or the bootstrap support (NJ/ML/MP). In bold are the Sardinian spatangoids. The bar and capital letters A (blue) and B (red) indicate the sequences of morphotype A and B, respectively.

oldest studies. In fact, many species have been established based on the description of a single specimen, often poorly described and/or illustrated.

Reviewing the sequence of fossils examined in this work, from a geologic/temporal point of view, the group of *Spatangus* (morphotype A) shows a path partially connected with *Sardospatangus* and probably with the Florida spatangid. The rest of the spatangids seems to form a different and interconnected group, having all the components of a very similar plastron.

In Figure 9, based on plastron schemes, we represent the hypothetical phylogenetic relationship between and within the groups and in Figure 10 their present geographical distribution.

In the present study, *S. purpureus* was found all around the coast of Sardinia at a wider depth ranging (from 22 to 183 m of depth), while *Propespatagus* was rare, found only in a few locations (range 86–181 m), generally coexisting with *S. purpureus* (Figure 1). Unlike in *S. purpureus*, *Propespatagus* shows a very thin and fragile test [observation also made by Mortensen (1913)] both for individuals of *Propespatagus inermis* from the Mediterranean and for specimens caught in different areas of the Pacific Ocean. This also applies to *S. mathesoni* of New Zealand (personal communication by Owen Anderson, NIWA). These details suggest the better adaptation to different environments than that of *S. purpureus*, but also a probable common ancestor in the second group (morphotype B — *Propespatagus*). It could therefore be hypothesized that morphotype B, *Propespatagus*, only partially (and coincidentally) shares the same environment as *S. purpureus*, and this would explain its low frequency in our fishing hauls. However, all these aspects need to be further addressed in dedicated studies in the future.

Concerning the genetic data, the newly generated sequences are the first genetic data for Spatangidae specimens caught in the Mediterranean Sea. In the past, DNA sequencing, in particular the COI DNA barcoding approach, has proved to be highly effective for echinoderm species discrimination, with the vast majority of species easily distinguished by their COI barcodes (Ward et al., 2008; Layton et al., 2016). In our study, nucleotide differences indicated the two morphotypes are molecularly distinct, and their degree of divergence is comparable to that of true valid species. Sequences from individuals of morphotype A can be identified as *S. purpureus*. The identification of specimens of morphotype A is solid, relying on both morphological appearance and sharing of molecular data with several sequences of *S. purpureus* deposited in GenBank/BOLD for multiple individuals and areas of the NE Atlantic Ocean. On the contrary, the identification of morphotype B specimens is more problematic. Molecular data seem to indicate that *Propespatagus* nov. sp. 1 is very close to *Propespatagus raschi*, differing only in a few nucleotide positions, the same degree of divergence that in previous studies was measured as the mean intraspecific value based on COI sequences (Ward et al., 2008; Layton et al., 2016). Special caution is required for the tentative molecular identification of morphotype B in this study since it was based on the only public available sequences for *P. raschi* from a single article (Stockley et al., 2005) and presumably a single individual caught in the NE Atlantic (United Kingdom), while, unfortunately, any sequence from *P. subinermis*, the second species known to occur

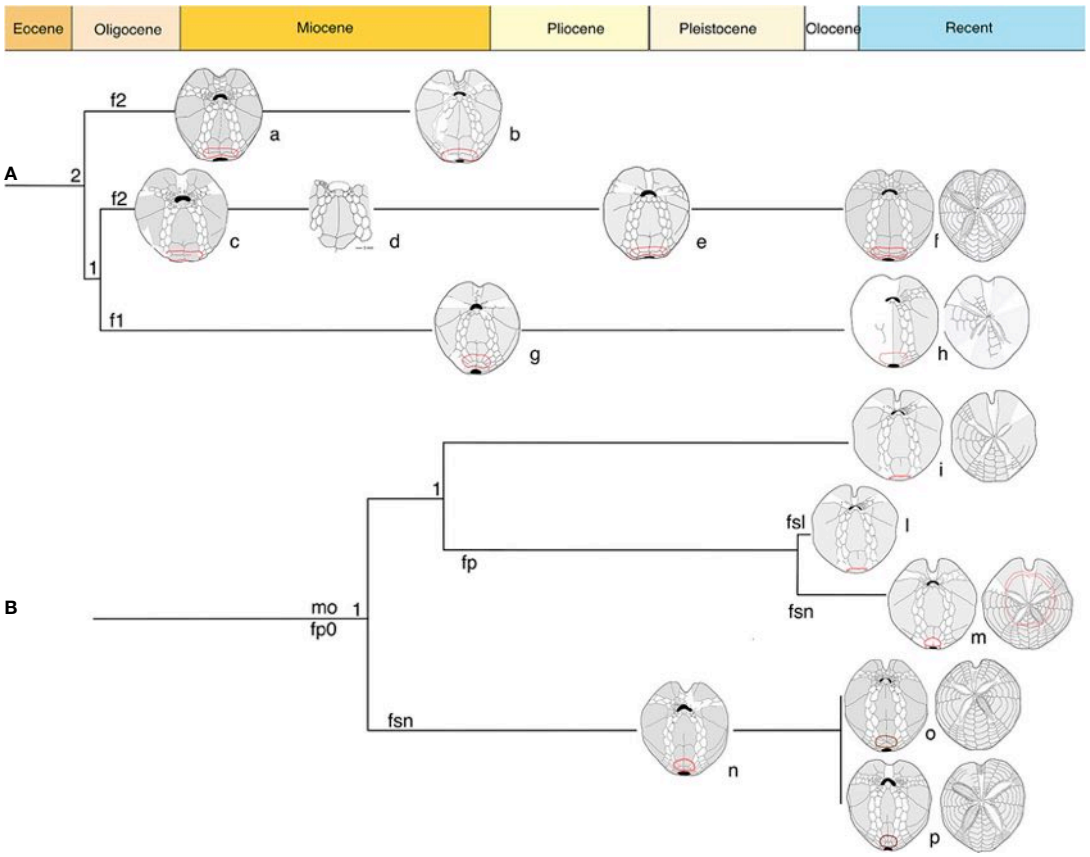

FIGURE 9
Diagram based on structural characters in adoral schemes. **(A)** Clade *Spatangus*/*Sardospatangus*; **(B)** clade *Propespatagus*, *Plethotaenia*, and other spatangids. Numbers: 1 = 1 plate; 2 = 2 plates per side of labrum. Letters: f1, f2 = fasciole with 1 or 2 indicating monolobed or bilobed. Other: fp = peripetal fasciole; fp0 = non- peripetal fasciole; fsl = large subanal fasciole; fsn = normal subanal fasciole. Specimens a– p, in order: *Sardospatangus caschilii*; *Sardospatangus saheliensis*; *Spatangus desmaresti*; *Spatangus* sp. 2 Ukraine; *Spatangus* cf. *purpureus*; *Spatangus purpureus*; Spatangidae sp. Florida; *"Spatangus" californicus*; *"Spatangus" mathesoni*; *Plethotaenia spatangoides*; *Plethotaenia angularis*; *Propespatagus subinermis*; *Propespatagus* sp. 1; *Propespatagus raschi*.

in the Mediterranean Sea, was available. Therefore, additional studies, combining morphological and molecular analyses, with extensive, dedicated sampling in the Atlantic and Mediterranean, are highly suggested to further investigate the differentiation between *Propespatagus* nov. sp. 1 (up to now documented only from the Mediterranean) and *S. raschi* (endemic to the NE Atlantic).

5 Description of the new genus and the species studied

This section is dedicated to the full description of the two species, as well as the diagnostic characters, useful to distinguish the new genus.

5.1 Systematic of Spatangidae

According to Kroh, 2020
Order Spatangoida L. Agassiz, 1840
Suborder Brissidina Kroh and Smith, 2010
Superfamily Spatangoidea Gray, 1825
Family Spatangidae Gray, 1825

5.1.1 Diagnostic characters of Spatangidae

Emended diagnosis (modified after Smith and Kroh, 2011): Spatangoidea with ethmolytic apical disc with four gonopores, flush or slightly depressed petals, pointed and closed distally; reduced pores adapically in the anterior column of the anterior paired petals; labrum, which does not extend beyond the second adjacent ambulacral plate; episternal plates equal and opposite; subanal fasciole present; rudimentary peripetalous fasciole may be present; periproct opening between plates 5.a.4 and 5.b.4 in the rear face; aboral face with scattered primary scrobiculate tubercles, variable in number, with the areolas indented but never very deep.

Genera included:

1) *Spatangus* Gray, 1825
2) *Plethothaenia* Clark, 1917
3) *Sardospatangus* Stara, Charbonnier et Borghi, 2018
4) *Propespatagus* gen. nov.

The diagnostic characters of the two species belonging to *Spatangus* and *Propespatagus* genera, on which this work is based, are described below.

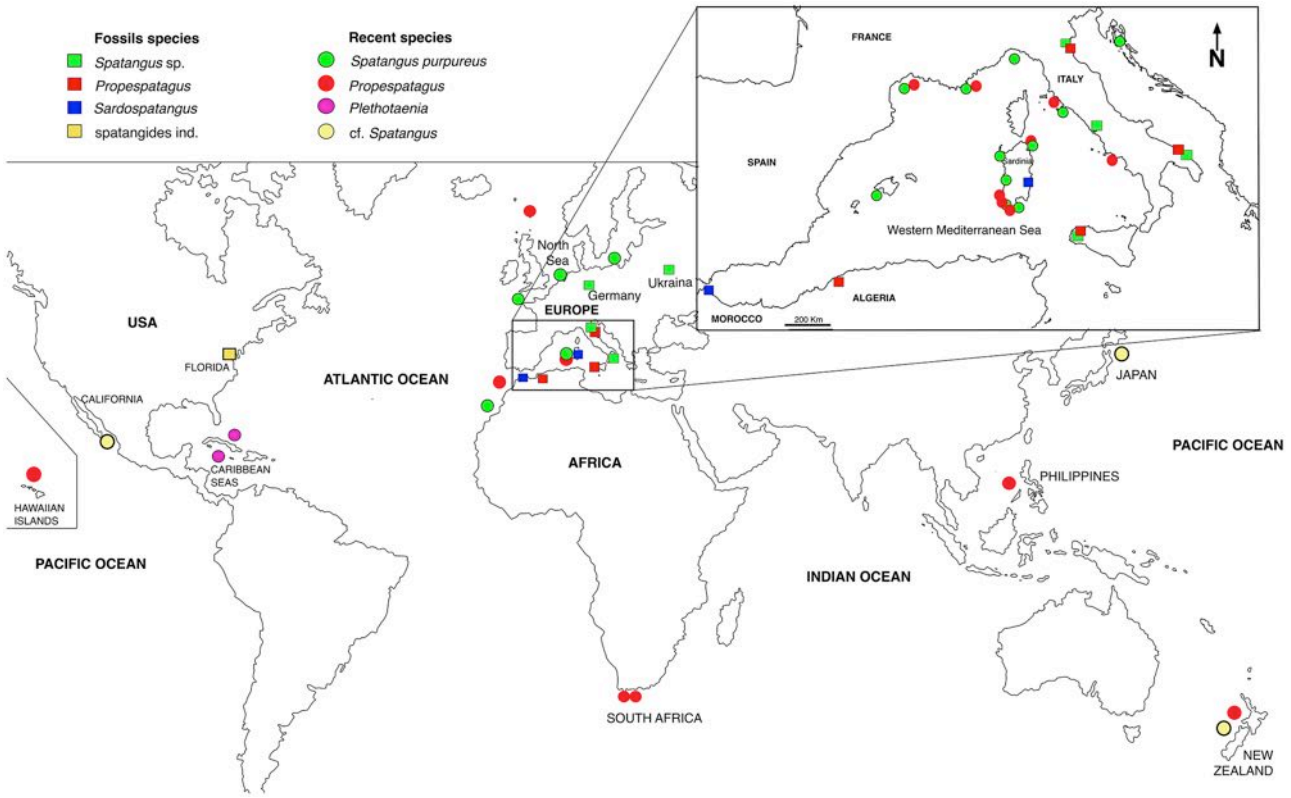

FIGURE 10
Geographical distribution of the analyzed species.

5.1.2 Diagnostic characters of the genus *Spatangus*

5.1.2.1 Description

Cordiform test with anterior groove; aboral surface domed; rounded margin, with slightly raised plastron; small apical disc, with a madreporic plate extending to the center and beyond the two posterior pores, where it tends to widen; narrow anterior ambulacrum with small simple isopores and phyllodes in peribuccal areas; the other ambulacra are petaloid adapically; slightly arched anterior paired petals with the pores of the anterior column adapically rudimentary or atrophied; the other pores large, paired and conjugated; posterior paired petals slightly expanded adapically and narrowing distally; medium- sized periproct, from subcircular to slightly elliptical, with greater horizontal diameter, open at the top on the posterior face, which is low and oblique and visible from below; small and kidney -shaped peristome, mostly covered by the labrum; labrum anvil- shaped, in contact with only one ambulacral plate on each side; finely tuberculated plastron, formed by wide and paired sternals, and wide episternal; heterogeneous aboral tubercles, with the primary ones scattered in the interambulacra in variable numbers, small and with shallow areoles; primary short spines; subanal fasciole, relatively thin and made up of very fine granules; it runs on large ambulacral plates that do not indent interambulacrum 5; the first two (sometime three) of these carry a subanal pore; the fasciole starts from the perradial suture between the two episternal plates, enclosing two large relief (bilobed) covered by tick tuberculation.

5.1.2.2 Species included:

S. purpureus Müller, 1776

S. desmaresti Goldfuss, 1829 (†)

?*Spatangus* sp. 2 Kroh, 2004 (†)

Many species of the European Miocene have been moved to the genus *Sardospatangus* Stara, Charbonnier et Borghi, 2018. Several other species need to undergo a systematic revision.

5.1.2.3 Distribution

Germany (Oligocene, Chattian); Ukraine (Miocene) and Plio-Pleistocene to Recent; Mediterranean and East Atlantic coasts from Senegal to North Sea.

Notably, in this work, the pedicellariae are not described because they are not considered diagnostic in the discrimination of the genera and species of Spatangidae; in the remarks in *Propespatagus* gen. nov. (ex *Spatangus* Auct.), moreover, we report only some characters that we consider diagnostic in this context. For any further information, see Mortensen (1913; 1951) and Néraudeau et al. (1998).

5.1.3 *S. purpureus* Müller, 1776

Figures 4A, 11A–F; Table 2

5.1.3.1 Essential synonymy

The complete list would be extremely wide and superfluous for the purpose of this work. However, for a historical reconstruction, we refer to Mortensen (1951) and, for an updated systematic situation, to WoRMS (World Register of Marine Species).

1776 —*S. purpureus* Müller p. 236, not figured, recent, coll. not indicated.

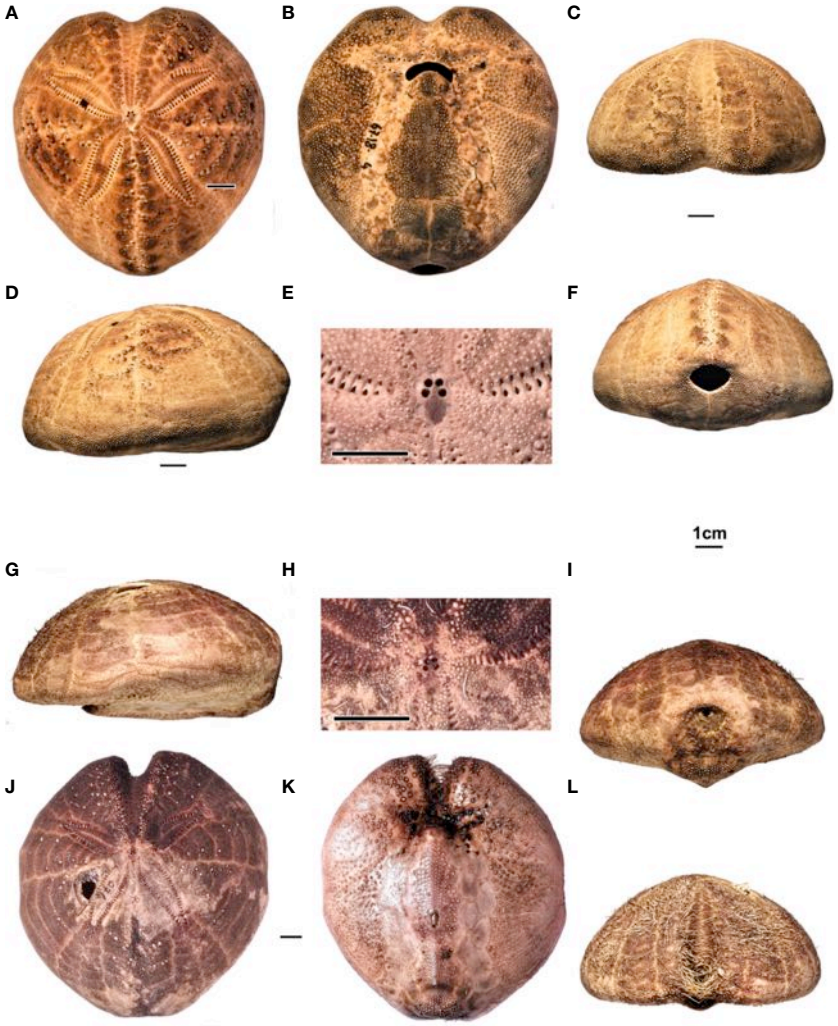

FIGURE 11
(A–F) *Spatangus purpureus*, Sardinia. Specimen MZ UNICA 067-MED18-4. In order, **(A–D)** aboral, adoral, frontal, and lateral views; **(E)** detail of the apical disc; **(F)** posterior view. **(G–L)** *Propespatagus* sp. 1, Sardinia. Specimen 074-MED18-2, holotype: **(G)** lateral, **(I)** posterior, **(K)** adoral, and **(L)** frontal views. Specimen 074-MED 18-1, **(J)** aboral view. Specimen MZ UNICA 085-MED18-1, **(H)** apical disc, detail.

1788— *S. purpureus* Müller p. 5, pl. 6, Figures 3–5, pl. 25, Figure 5.
1834— *S. purpureus* Müller, Blainville, p. 202, pl. 14, Figures 1–3.
1862— *S. purpureus*. Dujardin & Hupé, p. 607.
1862— *Spatangus meridionalis*. Dujardin & Hupé, p. 608.
1871 —*S. meridionalis*. Lütken, p. 138.
1872— *S. meridionalis*. Gray, p. 123.
1872— *S. purpureus*. A. Agassiz, p. 158.
1874— *S. purpureus*. Gauthier, p. 402.
1879— *S. purpureus*. Ludwig, p. 560.
1883— *S. purpureus*. Koehler, p. 127.
1891 —*S. purpureus*. Gregory, p. 42, 46.
1901 —*S. purpureus*. Mortensen, p. 29.
1905— *S. purpureus*. Döderlein, p. 199.
1906— *S. purpureus*. Döderlein, p. 260.
1906— *S. purpureus*. Checchia –Rispoli, p. 95.
1907— *S. purpureus*. Mortensen, p. 123.
1951— *S. purpureus* Müller, Mortensen, p. 10
1998— *S. purpureus* Müller, Néraudeau, Borghi & Roman, p. 6.
2005— *S. purpureus* Müller, Kroh, p. 150.
2018— *S. purpureus* Müller, Vadet & Nicolleau, pp. 106–108.
2018— *S. purpureus* Müller, Stara, Charbonnier & Borghi, p. 310.

5.1.3.2 Distribution

Fossils, from the Italian Plio-Pleistocene (Néraudeau et al., 1998; present study); recent, from Mediterranean to Atlantic European coasts (present study; Smith and Kroh, 2011; Stara et al., 2018; Vadet and Nicolleau, 2018).

5.1.3.3 Material studied

260 specimens fished along the coasts of Sardinia and deposited (30 specimens) at the MAC, inventoried IVM # and (230 specimens) at the MZ UNICA, inventoried MZ #; 2 fossil specimens from the Pliocene of Otranto, Puglia; 1 from Pliocene of Terre Rosse, Siena, Tuscany, and 1 from the Pleistocene-Holocene of Ostia, Lazio, Italy (MACPL 2015-2017).

5.1.3.4 Description

A species of *Spatangus* with the cordiform and domed test, rounded margin, relatively flat oral face, shallow anterior groove, labial plate in contact with a single ambulacral plate on each side, and wide contact with the sternals; thin sub-anal fasciole, laterally extended and bilobed.

In our sample, TL range from 64.5% to 123.5% TL and TW from 81% to 102.3% TL (Table 3).

The apical disc is positioned slightly anterior to the center (L8 average = 59.58% TL); ethmolytic, with the two anterior pores slightly closer together (Figure 7A).

Ambulacrum III is tight, with 27–29 minute and undifferentiated pores, and runs along the anterior groove progressively deepening, as it approaches the margin, where it reaches the maximum width. Other ambulacra petaloids adapically. The petaloids are relatively long and wide, despite their variability (L4 varies from 34.8 to 49.5% TL, an average of 42.4; L5 varies from 10 to 18.3% TL, mean of 13.3), and divergence between them an average of approximately 124 degrees. The pores of the anterior series become smaller or rudimentary (Figure 11A); adorally, each ambulacrum carries two series of five to six well-developed phyllodes that open into the peribuccal dimple (Figure 11B). Near the peristome, the plates are shorter than wide, but they progressively lengthen and then shorten toward the margin, where, however, they widen considerably (Figure 4A). The poriferous areas, in their central petaloid tract, measure approximately one-quarter of the interporiferous ones, which are devoid of tubercles; also the adoral portion carrying phyllodes is naked, while the marginal areas are covered by numerous small secondary tubercles. PLR is highly variable and ranges from 2.5 to 5.1 (average 3.6) in the sample examined (N 20). Paired posterior petaloids do not differ from the anterior by length and width (L6 ranges from 36.4 to 48.8% TL, average 41.9; L7 ranges from 9.3 to 17.8% TL), but the shape is generally less arched than the anterior ones with a divergence between them of approximately 62 degrees; the poriferous and interporiferous areas are similar to those of the paired frontal petals. On the adoral face, ambulacra I and V form a shower of elongated plates devoid of tubercles, which delimits the plastron without indenting it, where L15 measurements on average 38.5% TL (Figure 2). In Plates 6 and 7 there are evident two sub-anal pores, open within the perimeter of the fasciole.

All the interambulacra are amphiplacous, with the first plate extending up to the fourth (sometimes the fifth) plate of the anterior adjacent ambulacra and the third of the posterior paired ambulacra.

The labial plate extends only to the first adjacent ambulacral plate. The labrum protrudes anteriorly to partially cover the peristome, mushroom or anvil- shaped with the relatively wide base in contact with the two sternal plates (in our sample of *Spatangus*, L14 varies from 4% to 11% TL, with an average of 6.6% TL. The ratio between the averages of the length and width of the labrum in our sample is approximately 1.5. The sternal plates are broad (average L16 = approximately 30% TL; average L13 = 38.8% TL), with ratio L13/L16 = approximately 1.3, and do not restrict contact with the episternals, which normally falls at the fifth adjacent ambulacral plate (in our sample (n 128), it falls at the fourth plate of the ambulacrum V only in one case).

On the aboral interambulacra, tuberculation is heterogeneous and very variable; it consists of crenulate and perforate primary tubercles, whose areoles, which rarely exceed 2.4% TL in diameter, are arranged in straight lines or a "V"- shaped series along the plates of all the interambulacra (Figures 11A, D) and increase in size and diameter in the adapical direction.

On the adoral face, tuberculation is much more regular and less variable. All the interambulacra, including the plastron and the labrum, are covered by secondary perforated crenulate and scrobiculate tubercles (Figure 11B), which decrease in size as they approach the edge of the test. All ambulacra, indeed, are free from primary tubercles. Secondary tubercles are widespread especially at the edges of the anterior groove, while miliary tubercles are diffused and dense over the entire surface, except along the ambulacral poriferous areas.

The spines are articulate on the tubercles through thin but robust muscles anchored around the base of the stem and generally have the neck bent toward the posterior and/or lateral part of the body of the echinoid. The primary spines are thicker and longer than the secondaries; very variable in length, but normally are more than 15 mm long; they are found above all on the aboral surface and in a small part of the adoral portion of interambulacra 2 and 3, where they are shorter.

The secondary ones are densely distributed among the primaries and on the oral surface and generally less than 10 mm, mixed with the thin miliary spines, in analogy with the correspondent tubercles, as above described. However, in 110-mm- long individuals, we measured primary spines up to 34.5 mm long, equaling 31% TL (see also Figure S1).

On the adoral surface, there are also spatulate spines and hook-like curved spines, as on the labrum; each type of spine is clearly specialized in a specific function, but for further information, see Mortensen (1951).

In some individuals, 110 mm long, the oral secondary spines are up to 16.5 mm long, equaling approximately 15% TL.

The peristome is transverse and kidney-shaped and positioned approximately 25% TL far from the anterior margin on average (n 180). In living individuals, the stoma is surrounded by imbricated plates that open in the center.

The periproct is transverse and broad elliptic (Figure 11F) (mean L1 approximately 11% TL; mean L2 approximately 14% TL); it opens more or less high on the posterior face (on average 18% TL).

The subanal fasciole is thin and covered by a thick and very fine granulation, which carries very thin specialized spines (clavulae), with FW 1.21% TL on average; the pathway is long, with L17 measuring on average 43.7% TL (n 116), bilobed posteriorly and almost rectilinear anteriorly. The fasciole crosses the plates 5.a.3 and 5.b.3, then it passes in the ambulacrum I in position I.a.6 → 8, and returns to intercept interambulacrum 5 in 5.b.5 → 4 with a slight curve, goes back symmetrically in the other half of the test in 5.a.4 → 5, V.b.8 → 6, and finally rejoins the beginning of the loop (Figures 4A, 11B, F). Inside each lobe, there is a relief, highlighted by tubercles that decrease in size from the center to the periphery.

5.1.3.5 Remarks

The only fossils that should be accepted in the genus *Spatangus* and compared with *S. purpureus*, are *S. desmaresti* from the Oligocene of Germany and *Spatangus* sp. 2 from the Miocene of Ukraine. In the latter species, the labrum is in contact with only one adjacent ambulacral plate per part, but the fasciole is not visible; however,

from the close-up photos provided by Kroh (personal courtesy, August 2019), two distinct lobes, typical of *Spatangus* structure, seem visible. Many Plio-Pleistocene or Quaternary *Spatangus* specimens, which could be compared with living *S. purpureus*, have been recorded from many Mediterranean localities [see Néraudeau et al. (1998); Borghi (2012) and Stara et al. (2018)], but they will be re-evaluated when greater quantities of specimens will be available.

5.1.3.6 Distribution

Mediterranean, East, and North Atlantic from Senegal (GBIF, 2022) to Faroe Island and North seas (Mortensen 1951; Smith and Kroh, 2011). Other marine areas to be verified.

5.1.4 Diagnostic characters of the genus *Propespatagus*

Propespatagus gen. nov. Stara P., Melis R., Bellodi A., Follesa M.C., Corradini C., Carugati L., Mulas A., Sibiriu M., Cannas R.

Etymology: from *Propes* (Latin = close/similar) and *patagus* (name used by Jules Lambert, eminent French echinologist, to indicate some spatangoids).

Type species: MZ UNICA 074-MED18-2.

5.1.4.1 Diagnosis

Cordiform test with anterior groove, which can be very deep; aboral surface domed and pointed forward; rounded margin tending to narrow anteriorly, with keeled plastron; small ethmolytic apical disc, with four gonopores and a madreporic plate extending to the center and beyond the two posterior pores, where it tends to widen; narrow anterior ambulacrum with small simple isopores and phyllodes in peribuccal areas; the other ambulacra have flush petaloids; slightly arched anterior paired petals with the pores of the anterior column adapically rudimentary or atrophied; the other pores large, paired and conjugated; slightly expanded posterior paired petals adapically, narrowing distally; medium- sized periproct, from subcircular to slightly elliptical, with greater horizontal diameter, open at the top on the posterior face; small and kidney -shaped peristome, mostly covered by the labrum; labrum anvil- shaped, small, in contact with only one ambulacral plate on each side; finely tuberculated plastron, formed by long, narrow and paired sternals, and long and strongly posteriorly convergent episternals; heterogeneous aboral tubercles, with primary tubercles scattered in the interambulacra in variable numbers, small and with shallow areoles; primary short spines; small subanal fasciole, from cordiform to circular (slightly wider than long), thick and made up of very fine granules; the fasciole runs on narrow ambulacral plates, which strongly indent interambulacrum 5 at the rear, almost occluding it in some species; the first two of these plates carry a subanal pore; the fasciole starts from the perradial suture (in relief) between the two episternal plates, enclosing a single relief (monolobed) cover by tick tuberculation (see also Smith, 2013).

5.1.4.2 Species included

Propespatagus raschi (Lovén, 1869)
P. subinermis (Pomel, 1883)
P. paucituberculatus (A. Agassiz. & H.L. Clark, 1902)
P. capensis (Döderlein 1905)
P. inermis (Mortensen, 1913)
Propespatagus multispinus (Mortensen, 1925)
Propespatagus sp. 1, this work
Propespatagus sp. 2, this work

Other species, thus far classified as *Spatangus*, could belong to this new genus, but further studies and in particular molecular analysis are necessary to verify their correct taxonomic position.

5.1.4.3 Distribution

Fossil: from the Pliocene to the Holocene of Italy; living: from the Mediterranean and the Eastern Atlantic, the Shetland Islands, Pacific, and Indian Oceans.

5.1.5 *Propespatagus* sp. 1

Propespatagus sp. 1, Figures 4B; 11G–L, Table 2

Holotype: specimen MZ UNICA 074-MED18-2, illustrated in Figure 11.

Paratypes: MZ UNICA 028-MED18-1, 2; other specimens UNICA 074-MED18-1; MZ UNICA 078-MED-18-1 to 4; MZ UNICA 085-MED-18 1; MAC.IVM 350-1.

Diffusion. West Mediterranean, Sardinian coasts, and probable French coasts (Bonnet, 1926; DORIS, 2022).

5.1.5.1 Diagnosis

Species with domed test (thin and fragile), margin from rounded to narrow in the anterolateral region, with the oral face concave in the anterior part and convex in the posterior half, with plastron raised and keeled; very deep and narrow anterior groove; small labral plate in contact with only one ambulacral plate on each side, and with the two sternals longer than wide; thick, cordiform, heart- shaped or circular sub-anal fasciole, which runs on ambulacral plates 6, 7, and 8, which strongly indent inter-ambulacrum 5, forming an evident single central relief within the fasciole (monolobate), in the sub-periproctal region. Primary tubercles are scattered in the aboral part of all five interambulacra.

5.1.5.2 Description

Cordiform test with rounded margins, decidedly pointed anteriorly (Figure 11G), with narrow and close shoulders (L10 varies from 14.9 to 21.5% TL, average = 17.8% TL) and maximum height rear to apex on interambulacrum 5; test truncated posteriorly by an inclined face in an adoral sense, in the upper part of which opens the periproct (Figures 11G, I). Medium-large size (TL varies from 64.5 to 123 mm). The average width of the test (TW) is 92.94% TL.

The aboral face is raised posteriorly, with the maximum height (TH varies from 45 to 54.7% TL, average 51.14% TL) placed behind the apical disc (Figures 11G, J). The anterior groove is narrow and very deep, with the sinus L9 ranging from 9.3% to 11.9% TL (average = 10.71% TL).

The peristomial area is slightly sunken, on the oral face, which is slightly concave anteriorly, but with the labrum and the plastron in relief (Figures 11G, K).

The aboral tuberculation is scarce and heterogeneous, constituted by scrobiculate, crenulated, and perforated tubercles, small and with not very deep areoles; the test is covered with a

thick granulation that supports thin and short spines. The fasciole is small/medium- sized (L17 varies from 26.4 to 27.8, average 26.73% TL), but thick (average FW = 3.32% TL), and forms a subcircular or cordiform loop.

The apical disc is small (width approximately 1.8% TL) and slightly anterior to the center; L8 ranges from 57.6% to 64.4% TL (average approximately 61.8% TL), ethmolytic, with four gonopores; the anterior is slightly closer (Figure 11H).

Ambulacrum III with small and undifferentiated pores; it forms a deeper and wider anterior groove when approaching the margin with L9 that ranges from 9.3 to 11.9 (average of 10.7% TL); L10 approximately 18% TL (Figures 11L, K).

Paired anterior ambulacra petaloid in the aboral tract, mostly straight, slightly arched backward; relatively short and narrow; L4 ranges from 29.6% to 36.6% TL (average L4 = 33.3) and L5 ranges from 8.7% to 11.3% TL (average = 10% TL). The petals diverge on average at approximately 127 degrees; the pores of the anterior series become smaller adapically, and in many cases become rudimentary, but in smaller numbers than in *Spatangus* (Figure 11J); adorally, each ambulacrum carries two sets of five to six well-developed peribuccal phyllodes into the peristomial dimple. Near the peristome, the plates are shorter than wide, and they contain unipores surrounded by large periporal areas and gradually lengthen to then shorten toward the edge, where they widen again; the PLR is high and ranges from 3.7 to 4.5. The poriferous areas, in their central petaloid tract, are large about one-third of the interporiferous ones, which are devoid of tubercles; both the aboral and adoral tracts carrying phyllodes are bare, while the marginal areas are covered by numerous small secondary tubercles. The posterior paired ambulacra are longer (L6 ranges from 32.3% to 38.5% TL, average 35.7% TL) and relatively narrow (L7 ranges from 7.7% to 11.6% TL, average 9.7% TL); normally, they are more straight and slightly sharper than the anterior ones and diverge between them by approximately 60 degrees. The poriferous areas, in their central tract, measure approximately one-third of the interporiferous ones, which are devoid of tubercles. The non-petaloid aboral tract and the periplastronal tracts are devoid of tubercles, while the marginal tracts are covered by a dense secondary tuberculation. On the adoral face, ambulacra I and V form a more or less sub-parallel series of elongated plates that delimit the plastron (Figures 4B, 11K); in correspondence with the posterior part of the plastron, the relative ambulacral plates 6, 7, and 8 strongly indent the episternals (Figures 4B, 11K). In plates 6 and 7, there are evident pores within the perimeter of the fasciole.

The plastron is raised, keeled, and densely tuberculate as well as the labrum. The labrum protrudes anteriorly to cover a large part of the peristome; it is mushroom-shaped, short (average L12 = 6.2% TL) extending halfway through the adjacent ambulacral plates, with the base in short contact with the two sternal plates (average L14 = 4.3% TL). The sternal plates are narrow and long (average L13 = 38.5% TL and average L16 = 24.3% TL, with the ratio between L13/L16 approximately 1.6). The suture between the sternal and episternal plates falls normally at the fifth adjacent ambulacral plate. Posteriorly, the episternals are strongly indented by the ambulacral plates, so much as to occlude, in some specimens, interambulacrum 5; within the perimeter of the subanal fasciole, the episternals form a central tuberculate relief (Figures 11I, K).

The primary tuberculation is heterogeneous and scarce on the aboral interambulacral side (Figure 11J); the primary tubercles are small, crenulated, and perforated, with the shallow areoles, which rarely exceed 2% TL in diameter; they are arranged singly or in short horizontal lines, obliquely on the plates of the interambulacra, more abundant adapically. The primary spines are rather short, not exceeding 15% TL; they are thin and striped; the secondary ones do not exceed 7% TL, are very thin, and cover the entire surface, interspersed with the miliaries.

All the interambulacra, in the oral face, including the plastron and the labrum, are covered by secondary perforated and scrobiculate tubercles, which diminish in size as they approach the edges of the plates and toward the margin of the test (Figure 11K). Also, the adoral tract of the ambulacrum III has secondary tubercles, while the periplastronal tracts of the ambulacra are naked. The fasciole is covered by a very fine granulation that carries very thin clavulae; the rest of the tuberculate surface within the fasciole has spines no longer than 0.7% TL and is very thin.

The peristome is transverse, small, and kidney-shaped, approximately 23% TL far from the anterior border (Figure 11K). In living individuals, the stoma is surrounded by imbricate plates that leave a central opening and is covered for the most part by the labrum.

The periproct is small (L1 measuring on average 8.5% TL) and is slightly elliptical transverse (mean L2 = 11.5% TL) and opens between plates 5.a.4/5 and 5.b.4/5 (Figure 11I).

The fasciole is thick, with a short path that varies from roundish to cordiform, with L17 ranging from 25.4% to 27.7% TL (on average 26.7% TL). The pathway starts from the center of the two episternal plates, which is positioned along their perradial suture. The formula is 5.a.3 and 5.b.3; then it runs on the ambulacra in the I.a.6 → 9 position and then returns to intercept the interambulacrum at 5.b.4, drawing a slight indentation in the presence of a subanal dimple, to continue symmetrically in the other half of the test in 5.a.4, V.b.9 → 6, to then close the path rejoining with the start of the loop (Figures 4B, 11I, K). Inside the loop drawn by the fasciole (monolobate), there is one relief, highlighted by tubercles larger in the center, which decrease in size as they approach the fasciole.

5.1.5.3 Remarks

Propespatagus sp. 1 (Figures 4B, 11J) differs from *P. inermis* (Figure 5B) in having a deeper anterior sinus (mean L9 = 10.7, versus a maximum of 8.7% TL) and primary tubercles widespread in all interambulacra, while *P. inermis* is completely tubercle-free in interambulacra 1 and 4. *Propespatagus paucitubercolatus* (Figure 5C) is very close morphologically to the Sardinian species, since it has a similar anterior sinus, but it differs in the primary tuberculation, absent in the two interambulacra 1 and 4, and in the length of the petals, which are longer [mean L6 = 41% (n 2) against TL 35.7 (n 10)]; however, given the geographical distance and the presumed environmental difference and pending molecular analyses, it is treated here as a distinct species.

P. sp. 1 differs from *P. raschi*, in the lower height (51 against 60% TL), in its shorter petals (average L6 = 35.7 against 42% TL) (Figure 5E), and in the size of the fasciole (average L17 = 26.7 *vs.* 23% TL and FW thicker).

P. sp. 1 differs from *P. capensis* (species very close to *P. raschi*) in the lower test height (TH = 51, against 60% TL), in having a different

number of spines (see raschi), and in the lack of tubercles primary on the aboral extrapetal ambulacral surfaces. *P.* sp. 1 also differs from *P. multispinus*, with shorter spines (15% TL *vs*. 27% TL) and much fewer in number.

Finally, *P.* sp. 1 clearly differs from *P. raschi* and *P. capensis* in having a much deeper sinus (Figures 5E, F) and much smaller petals. The set of characters, as also visible in Figures 5E, F, clearly detaches the two Atlantic species from the Sardinian ones.

For complete descriptions of *P. raschi*, *P. capensis*, *P. paucituberculatus*, and *P. multispinus*, see Mortensen (1951).

6 Conclusion

The availability of a significant number of studied specimens allowed us to clarify the variability limits of some important diagnostic characters, enhancing the possibility to discriminate species and genera among the Spatangidae.

The use of all these characters in the morphometric and morpho-structural analyses, and the appropriate genetic analyses performed, allowed us to clarify the taxonomical relationships within the family Spatangidae, distinguishing four genera. This method aims to lay the foundations also for the specific distinction within this and other spatangoid families.

Data availability statement

The data presented in the study are deposited in the GenBank® repository (Sayers et al., 2022), accession number OP361060-OP361073; OP359422- OP359435. Additional details on DNA sequences are found in the article/Supplementary Material.

Author contributions

PS: Conceptualization, Methodology, Formal Analysis, Data curation, Visualization, Writing- Original draft preparation, Writing - Review & Editing. RM: Investigation, Formal Analysis, Data curation, Visualization, Writing- Original draft preparation. AB: Investigation, Formal Analysis, Writing- Original draft preparation. MCF: Resources, Writing - Review & Editing. CC: Supervision, Writing - Review & Editing. LC: Writing - Review & Editing, AM: Formal Analysis, Writing- Original draft preparation, MS: Investigation, Formal Analysis. RC: Methodology, Formal Analysis, Visualization, Writing- Original draft preparation, Writing - Review & Editing, Resources. All authors contributed to the article and approved the submitted version.

Acknowledgments

We thank all contributors to this research. In particular, we are grateful to all the participants in the scientific surveys, as well as the crew of each research vessel for their sampling effort: Andreas Kroh (the NHMW) Wien, Austria; Sylvain Charbonnier (MNHNF) Paris, France; Claudia di Somma and Andrea Travaglini (SZN) Naples, Italy; Anderson Owen (NIWA), Wellington, New Zealand; and Luigi Sanciu (MAC) Masullas, Oristano, Sardinia, Italy. Also heartfelt thanks to the paleontologist researchers (Fabio Ciappelli (Private collection), Prato, Tuscany; Enrico Borghi (Private Collection), Modena, Emilia Romagna; and Giuseppe Carone (Paleontological Museum of Vibo Valentia), Calabria, Italy), who provided us with precise indications on paleontological localities and their collected specimens.

Conflict of interest

The authors declare that the research was conducted in the absence of any commercial or financial relationships that could be construed as a potential conflict of interest.

Publisher's note

All claims expressed in this article are solely those of the authors and do not necessarily represent those of their affiliated organizations, or those of the publisher, the editors and the reviewers. Any product that may be evaluated in this article, or claim that may be made by its manufacturer, is not guaranteed or endorsed by the publisher.

Supplementary material

The Supplementary Material for this article can be found online at: https://www.frontiersin.org/articles/10.3389/fmars.2023.1033710/full#supplementary-material

References

Anderson, M. J., and Willis, T. J. (2003). Canonical analysis of principal coordinates: a useful method of constrained ordination for ecology. *Ecology* 84 (2), 511–525. doi: 10.1890/0012-9658(2003)084[0511:CAOPCA]2.0.CO;2

Baker, A. N., and Rowe, F. W. E. (1990). Atelostomatid Sea urchins from Australian and new zeland waters (Echinoidea: Cassiduloida, holasteroida, spatangoida, neolampadoida. *Invertebrate. Taxonomy.* 4, 281–316. doi: 10.1071/IT9900281

Bonnet, A. (1926). Document pour servir à l'étude de la variation chez les Échinides. v. variations du test chez le *Spatangus purpureus*. *Bull. l'Institut. Océanographique. Monaco.* 23, 1–27.

Borghi, E. (2012). Il genere Spatangus (Echinoidea) nel Langhiano dell'Appennino reggiano. *Notiziario della Società Reggiana di Scienze Naturali. Reggio Emilia* 2010, 43–61.

Borri, M., Righini, P., and Piras, A. (1990). Fauna echinologica dei fondi molli dell'alto tirreno e note sulle biocenosi relative. *Atti. Della. Società. Italiana. di. Sci. Naturali. e del. Museo. Civico. di. Storia. Naturale. di. Milano.* 131 (26), 377–410.

Bucklin, A., and Frost, B. W. (2009). Morphological and molecular phylogenetic analysis of evolutionary lineages within clausocalanus (Copepoda: Calanoida). *J. Crustacean. Biol.* 29 (1), 111–120. doi: 10.1651/07-2879.1

Chesher, R. H. (1968). The systematics of sympatric species in West Indian spatangoids: A revision of the genera *Brissopsis, Plethotaenia, Paleopneustes*, and *Saviniaster*. *Stud. Trop. Oceanogr.* 7, 1–168, pls 1-35.

Chippindale, P. T., and Wiens, J. J. (1994). Weighting, partitioning, and combining characters in phylogenetic analysis. *Syst. Biol.* 43 (2), 278–287. doi: 10.2307/2413469

Clark, H. L. (1917). Hawaiian And other pacific echini / by Alexander agassiz and Hubert Lyman Clark. *Mem. Mus. Comp. Zool.* 46 (2), 234.

Clarke, K. R., and Gorley, R. N. (2015). *Primer v7: user manual/tutorial* (Plymouth: PRIMER-E Ltd).

Collin, R., Venera-Pontón, D. E., Driskell, A. C., Macdonald, K. S., Geyer, L. B., Lessios, H. A., et al. (2020). DNA Barcoding of echinopluteus larvae uncovers cryptic diversity in neotropical echinoids. *Invertebrate. Biol.* 139 (2), e12292. doi: 10.1111/ivb.12292

DORIS (2022) *Spatangus subinermis*. Available at: https://doris.ffessm.fr/Especes/Spatangus-subinermis-Spatangue-profond-d-Europe-1293/(rOffset)/0. [accessed August 27, 2022]

Filander, Z., and Griffiths, C. (2017). Illustrated guide to the echinoid (Echinodermata: Echinoidea) fauna of south Africa. *Zootaxa* 4296, 1–72. doi: 10.11646/zootaxa.4296.1.1

GBIF (2022). *Spatangus purpureus* O.F.Müller, 1776 in GBIF Secretariat (2022). GBIF Backbone Taxonomy. Checklist dataset. https://doi.org/10.15468/39omei [accessed https://via GBIF.org on August 27, 2022]

Gray, J. E. (1825). An attempt to divide the echinida, or Sea eggs, into natural families. *Ann. Philos. New series.* 10, 423–431.

Hammer, Ø., Harper, H. A. T., and Ryan, P. D. (2001). PAST: Paleontological statistics software package for education and data analysis. *Palaeontol. Electronica.* 4(1), 4. Available at: http://palaeo-electronica.org/2001_1/past/issue1_01.htm.

Huelsenbeck, J. P., Bull, J. J., and Cunningham, C. W. (1996). Combining data in phylogenetic analysis. *Trends Ecol. Evol.* 11 (4), 152–158. doi: 10.1016/0169-5347(96)10006-9

Kroh, A. (2005). *Echinoidea neogenica. catalogus fossilium austriae. band 2* (Wien: Verlag der Österreichischen Akademie der Wissenschaften) Vienna, 210 p., 82

Kroh, A. (2007). Hemipatagus, a misinterpreted loveniid (Echinodermata: Echinoidea). *J. Syst. Palaeontol.* 5 (2), 163–192. doi: 10.1017/S1477201906002021

Kroh, A. (2020). "Phylogeny and classification of echinoids," in *Sea Urchins: Biology and ecology*. Ed. J. Lawrence (Cambridge: Academic Press), 1–17. doi: 10.1016/B978-0-12-819570-3.00001-9

Kroh, A., and Mooi, R. (2022) *World echinoidea database. spatangus Gray*. Available at: https://www.marinespecies.org/aphia.php?p=taxdetails&id=123430 (Accessed 2022-07-26).

Kroh, A., and Smith, A. B. (2010). The phylogeny and classification of post-Palaeozoic echinoids. *J. Syst. Palaeontol.* 8 (2), 147–212. doi: 10.1080/14772011003603556

Kumar, S., Stecher, G., and Tamura, K. (2016). MEGA7: Molecular evolutionary genetics analysis version 7.0 for bigger datasets. *Mol. Biol. Evol.* 33 (7), 1870–1874. doi: 10.1093/molbev/msw054

Lachkhem, L., and Roman, J. (1995). Les échinoïdes irréguliers (néognathostomes et spatangoïdes) du messinien de melilla (Maroc septentrional). *Annales. Paléontol. (Vertébrés-Invertébrés).* fasc. 4, vol. 81, 247–278.

Lambert, J. (1915). Description des échinides des terrains néogènes du bassin du rhône. *Mémoires. la. Société. Paléontol. Suisse.* 41, 155–240.

Layton, K. K. S., Corstorphine, E. A., and Hebert, P. D. N. (2016). Exploring Canadian echinoderm diversity through DNA barcodes. *PloS One* 11 (11), 16. doi: 10.1371/journal.pone.0166118

Littlewood, D. T., and Smith, A. B. (1995). A combined morphological and molecular phylogeny for sea urchins (Echinoidea: Echinodermata). *Philos. Trans. R. Soc. Lond. B. Biol. Sci.* 347 (1320), 213–234. doi: 10.1098/rstb.1995.0023

Lovén, S. (1874). Etudes sur les echinoidees. *Kongelige. Svenska. Vetenskaps-Akademiens. Handlingar.* 11, 1–91.

McNamara, K. J. (1982). Heterochrony and phylogenetic trends. *Paleobiology* 8 (2), 130–142. doi: 10.1017/S0094837300004474

McNamara, K. J. (1987). Plate translocation in spatangoid echinoids: its morphological, functional and phylogenetic significance. *Paleobiology* 13 (3), 312–325. doi: 10.1017/S0094837300008897

McNamara, K. J. (1988). "Heterochrony and the evolution of echinoids," in *Echinoderm phylogeny and evolutionary biology*. Eds. C. R. C. Paul and A. B. Smith. (Oxford: Oxford University Press), 111–119.

McNamara, K. J. (1989). The role of heterochrony in the evolution of spatangoid echinoids. *Geobios* 22, 283–295. doi: 10.1016/s0016-6995(89)80029-4

Mongiardino Koch, N. (2021). Exploring adaptive landscapes across deep time: A case study using echinoid body size. *Evolution* 75(6), 1567–1581. doi: 10.1111/evo.14219.

Mongiardino Koch, N., Coppard, S. E., Lessios, H. A., Briggs, D. E.G., Mooi, R., and Rouse, G. W. (2018). A phylogenomic resolution of the sea urchin tree of life. *BMC Evol Biol* 18(1), 189. doi: 10.1186/s12862-018-1300-4.

Mongiardino Koch, N., and Thompson, J. R. (2021). A total-evidence dated phylogeny of echinoidea combining phylogenomic and paleontological data. *Syst. Biol.* 70(3), 421–439. doi: 10.1093/sysbio/syaa069

Mongiardino Koch, N., Thompson, J. R., Hiley, A. S., McCowin, M. F., Armstrong, A. F., Coppard, S. E., et al. (2022). Phylogenomic analyses of echinoid diversification prompt a re-evaluation of their fossil record. *Elife* 11. doi: 10.7554/eLife.72460.

Mortensen, T. (1907). *The Danish ingolf-expedition 1895–1896. Echinoidea, pt. 1* (Copenhagen: Bianco Luno).

Mortensen, T. (1913). Die echiniden des mittelmeeres. eine revidierte ubersicht der im mittelmeere lebended echiniden, mit bemerkungen uber neue oder weniger bekannte formen. *Zool. Station zu Neapel. zugleich. ein. Repertorium. fur. Mittelmeerkunde.* 21, 1. Berlin, VERLAG VON R. FRIEDLÄNDER & SOHN

Mortensen, T. (1948). Contributions to the Biology of the Philippine Archipelago and adjacent regions. *Report on the Echinoidea collected by the United States Fisheries Steamer "Albatross" during the Philippine Expedition, 1907-1910. Part 3: The Echinoneidae, Echinolampidae, Clypeastridae, Arachnidae, Laganidae, Fibulariidae, Urechinidae, Echinocorythidae, Palaeostomatidae, Micrasteridae, Palaepneustidae, Hemiasteridae, and Spatangidae*. Smithsonian Institution, United States National Museum Bulletin Bulletin. Washington, US. 100, 93–140.

Mortensen, T. (1951). *A monograph of the Echinoidea. V, 2. Spatangoida II. Amphisternata II. Spatangidae, Loveniidae, Pericosmidae, Schizasteridae, Brissidae* (Copenhagen: C. A. Reitzel).

Néraudeau, D., Borghi, E., and Roman, J. (1998). Le genre d'échinide *Spatangus* dans les localités du pliocène et du pléistocène d'Émilie (Italie du nord). *Annales. Paléonol.* 84, 3–4. 243-264.

Néraudeau, D., Dudicourt, J.-C., Boutin, F., Ceulemans, L., and Nicolleau, P. (2010). Les Spatangus du miocène et du pliocène de l'Ouest de la France. *Annales. Paléontol.* 96 (4), 159–170. doi: 10.1016/j.annpal.2011.05.001

Palumbi, S. R., Martin, A., Romano, S., McMillan, W. O., Stice, L., and Grabowski, G. (1991). *The simple fool's guide to PCR, version 2.0* (Honolulu: Department of Zoology and Kewalo Marine Laboratory University of Hawaii).

Risso, (1826). *Histoire naturelle des principales productions de l'Europe mèridionale et particulièrement de celles des environs de nice et des alpes maritimes* (Paris - Strasbourg, G. Levrault).

Ronquist, F., Teslenko, M., van der Mark, P., Ayres, D. L., Darling, A., Höhna, S., et al. (2012). MrBayes 3.2: efficient Bayesian phylogenetic inference and model choice across a large model space. *Syst. Biol.* 61 (3), 539–542. doi: 10.1093/sysbio/sys029

Sayers, E. W., Bolton, E. E., Brister, J. R., Canese, K., Chan, J., Comeau, D. C., et al. (2022). Database resources of the national center for biotechnology information. *Nucleic Acids Res* 50(D1), D20–d26. doi: 10.1093/nar/gkab1112.

Schultz, H. (2009). *Sea Urchins II: Worldwide irregular deep water species* (Hemdingen: Heinke & Peter Schultz Partner Scientific Publications), 501–849, ISBN: .

Serafy, D. K., and Fell, F. J. (1985). *Marine flora and fauna of the northeastern united states. Echinodermata: Echinoidea* (U.S. DEPARTMENT OF COMMERCE: NOAA Technical Report NMFS).

Shin, S. (2013). A newly recorded Sea urchin (Echinoidea: Spatangoida: Spatangidae) from geomundo island, Korea. *Anim. Syst. Evol. Diversity* 29 (4), 308–311. doi: 10.5635/ased.2013.29.4.308

Smith, A. B. (2005). "Growth and form in echinoids. the evolutionary interplay of plate accretion and plate addition," in *Evolving form and function: Fossils and development. proceedings of a symposium honoring Adolf seilacher for his contributions to paleontology, in celebration of his 80th birthday*. Ed. D. E.G. Briggs(New Haven, Connecticut USA, Peabody Museum of Natural History), 181–195.

Smith, A. B. (2013). "Key to genera of spatangidae," in *The echinoid directory*. Eds. A. B. Smith and A. Kroh (World Wide Web Electronic publication.). The Natural History Museum, London. Available at: http://www.nhm.ac.uk/research-curation/research/projects/echinoid-directory/taxa/key.jsp?id=297. [Accessed August 27, 2022].

Smith, A. B., and Kroh, A. (2011). *The echinoid directory* (World Wide Web electronic publication). The Natural History Museum, London. Available at: http://www.nhm.ac.uk/research-curation/projects/echinoid-directory. [Accessed August 27, 2022].

Smith, A. B., Littlewood, D. T. J., and Wray, G. A. (1995). Comparing patterns of evolution: Larval and adult life history stages and ribosomal RNA of post-Palaeozoic echinoids. *Philos. Transactions.: Biol. Sci.* 349 (1327), 11–18.

Smith, A. B., Pisani, D., Mackenzie-Dodds, J. A., Stockley, B., Webster, B. L., and Littlewood, D. T. (2006). Testing the molecular clock: molecular and paleontological estimates of divergence times in the echinoidea (Echinodermata). *Mol. Biol. Evol.* 23 (10), 1832–1851. doi: 10.1093/molbev/msl039

Smith, A. B., and Stockley, B. (2005). Fasciole pathways in spatangoid echinoids: a new source of phylogenetically informative characters. *Zool. J. Linn. Soc.* 144 (1), 15–35. doi: 10.1111/j.1096-3642.2005.00161.x

Spedicato, M. T., Massutí, E., Mérigot, B., Tserpes, G., Jadaud, A., and Relini, G. (2019). The MEDITS trawl survey specifications in an ecosystem approach to fishery management. *Sci. Marina.* 83 (S1), 9–20. doi: 10.3989/scimar.04915.11X

Stara, P., Borghi, E., and Kroh, A. (2016). Revision of the genus mariania (Echinoidea) with the description of two new species from the Miocene of Italy. *Bull. Geosci.* 91 (1), Stara65–88. doi: 10.3140/bull.geosci.1576

Stara, P., Charbonnier, S., and Borghi, E. (2018). Redefinition of prospatangus thieryi Lambert 1909 (Echinoidea, spatangoida), in sardospatangus nov. gen. with two new species from Sardinia, Italy. *Annales. Paleontol.* 104 (4), 309–327. doi: 10.1016/j.annpal.2018.10.001

Stockley, B., Smith, A. B., Littlewood, T., Lessios, H. A., and Mackenzie-Dodds, J. A. (2005). Phylogenetic relationships of spatangoid sea urchins (Echinoidea): taxon sampling density and congruence between morphological and molecular estimates. *Zool. Scripta.* 34 (5), 447–468. doi: 10.1111/j.1463-6409.2005.00201.x

Sumida, P. Y. G., Tyler, P. A., Thurston, M. H., and Gage, J. D. (2001). Early post-metamorphic ontogenesis of deep-sea spatangoids (Echinoidea, spatangoida) of the NE Atlantic ocean. *Invertebrate. Biol.* 120 (4), 378–385. doi: 10.1111/j.1744-7410.2001.tb00046.x

Swofford, D. L. (2003). *PAUP*. phylogenetic analysis using parsimony (* and other methods). version 4* (Sunderland, Massachusetts, Sinauer Associates).

Thompson, J. R., Erkenbrack, E. M., Hinman, V. F., McCauley, B. S., Petsios, E., and Bottjer, D. J. (2017). Paleogenomics of echinoids reveals an ancient origin for the double-

negative specification of micromeres in sea urchins. *Proc Natl Acad Sci U S A* 114(23), 5870–5877. doi: 10.1073/pnas.1610603114.

Thompson, J. D., Higgins, D. G., and Gibson, T. J. (1994). CLUSTAL W: improving the sensitivity of progressive multiple sequence alignment through sequence weighting, position-specific gap penalties and weight matrix choice. *Nucleic Acids Res.* 22 (22), 4673–4680. doi: 10.1093/nar/22.22.4673

Tortonese, E. (1965). *Echinodermata Fauna d'Italia Volume VI*. 186 fig., 424 pp Bologna: Edizioni Calderini.

Vadet, A., and Nicolleau, P. (2018). Evolution des spatangues. *Annales de la Société d'Histoire Naturelle du Boulonnais*. Tome XVII. 1, 4, 128pp.

Ward, R. D., Holmes, B. H., and O'Hara, T. D. (2008). DNA Barcoding discriminates echinoderm species. *Mol. Ecol. Resour.* 8 (6), 1202–1211. doi: 10.1111/j.1755-0998.2008.02332.x

Ziegler, A., Stock, S., Menze, B., and Smith, A. (2012). "Macro- and microstructural diversity of sea urchin teeth revealed by large-scale micro-computed tomography survey," in *Proc. SPIE 8506, Developments in X-Ray Tomography VIII*, 17 October 2012, Vol. 85061G. doi: 10.1117/12.930832